

KfK 4851
März 1991

Monte Carlo Calculations with the MCNP Code for Investigations of Neutron and Photon Transport at the ASDEX Upgrade Tokamak

G. Fieg
Institut für Neutronenphysik und Reaktortechnik
Projekt Kernfusion

Kernforschungszentrum Karlsruhe

KERNFORSCHUNGSZENTRUM KARLSRUHE
Institut für Neutronenphysik und Reaktortechnik
Projekt Kernfusion

KfK 4851

Monte Carlo Calculations with the MCNP Code for
Investigations of Neutron and Photon Transport
at the ASDEX Upgrade Tokamak

G. Fieg

Kernforschungszentrum Karlsruhe GmbH, Karlsruhe

Als Manuskript gedruckt
Für diesen Bericht behalten wir uns alle Rechte vor

Kernforschungszentrum Karlsruhe GmbH
Postfach 3640, 7500 Karlsruhe 1

ISSN 0303-4003

Abstract

The Los Alamos MCNP Monte Carlo code has been applied to model the ASDEX Upgrade tokamak at the Max-Planck-Institute at Garching for a variety of different plasma diagnostic methods. In addition to this the neutron activation of some structural materials of the tokamak machine has been investigated. Furthermore the transport of photon radiation and resulting dose rates at some strategic points has been studied by applying the photon portion of MCNP. This report describes the neutron activation and photon transport calculations and resulting gamma dose levels at some strategic points near the tokamak.

Monte Carlo Rechnungen mit dem MCNP Code zum Neutronen- und Photonentransport im ASDEX-Upgrade Tokamak

Zusammenfassung

Der Los Alamos Monte Carlo Code MCNP wurde verwendet, um den ASDEX-Upgrade Tokamak am Max-Planck-Institut für Plasmaphysik in Garching für verschiedene Methoden von Plasma-Diagnostiken zu modellieren. Weiterhin wurde die Neutronenaktivierung einiger Strukturmaterialien untersucht und mit Hilfe von MCNP Photonentransportrechnungen die Strahlungsdosen an einigen strategischen Orten ermittelt. Dieser Bericht beschreibt die Untersuchungen zur Neutronenaktivierung und Photonentransportrechnungen sowie die daraus resultierenden Gammastrahlungsdosen.

Table of Contents	Page
1. Introduction	1
2.The MCNP Simulation Model	1
2.1 Topology of the Model	1
2.2 Material Compositions, Masses and Data Files	2
2.3 Neutron Source Distribution	3
2.4 Photon Source Distribution	3
3.Neutron Activation Calculations	4
3.1 Structures,Isotopes and Activation Cross Sections	4
3.2 Neutron Spectra from d-d and d-t Plasma Neutrons	4
3.3 Neutron Activation and Activities	5
4.Photon Transport Calculations and Dose Rates	5
5.Summary and Conclusions	6
6.References	7
7.Appendix A	9

1. Introduction

At the Max-Planck-Institute for Plasmaphysics at Garching a new tokamak, ASDEX Upgrade, has recently been constructed with the main object to study plasma-wall interaction phenomena. Compared to the former ASDEX machine the maximum plasma current will be 2 MA, that is four times higher at ASDEX Upgrade /1/. The plasma discharges can be kept up to 10 seconds. Experiments will be performed with light hydrogen, mixtures of deuterium and light hydrogen and with deuterium plasmas. In addition to the ohmic heating phase the neutral beam injection and ion cyclotron resonance heating (ICRH) up to 15 MW are foreseen for discharges up to 10 seconds.

The maximum neutron production in deuterium plasmas with additional ICRH-heating can amount 10^{18} neutrons per hour in the average. The majority of these neutrons is in the 2.5 MeV energy region due to d-d-reactions, but also a certain amount of 14.7 MeV neutrons will be emitted due to the burnup of tritons which are produced in the d(d,t)p reaction branch. This neutron emission leads to activation of the tokamak machine structures and also of the argon content in the air inside the experimental hall. Activation in the structures is predominantly due to radiative capture. In some cases, especially with high energy d-t neutrons also (n,p)-reactions in the different structure materials will lead to radioactive isotopes of relatively long half times.

To assess radiation levels in the tokamak surrounding due to neutron activation the transport of photon radiation has also to be investigated in addition to neutron transport. The MCNP Monte Carlo code /2/ incorporates a portion for photon transport, which has been used for this purpose.

2. The MCNP Simulation Model

2.1 Topology of the Model

This chapter describes the modeling of the tokamak geometry. Due to symmetry considerations, only one octant needs to be modeled. The two vertical planes which form the borders to the remaining tokamak are reflecting surfaces for both neutron and photon particles. This feature simulates the total 2π geometry, see figs. 1 and 2. This model, from here on called AUG03, describes the topology including one large and one small port of the tokamak. A toroidal field coil is situated in between the ports and two halves of toroidal field coils border the reflecting planes. The center structures (column, center poloidal field coil, the inner toroidal field coils, vacuum vessel and carbon tiles) are of cylindrical geometry. Inside the vacuum vessel the two passive copper stabilizers are shown. They are needed to calculate the Co-63 (n, γ)-activation. The upper and lower divertor structures are modeled as horizontal plates close to the vacuum vessel.

The outer toroidal structures around the vacuum zone (vacuum vessel, toroidal field coils, shear compression structures ("Kippstruktur"), ports and poloidal field coils together with the steel structure ("Stützstruktur")) are modeled as close as possible to the real geometry using plane, cylindrical and conical surfaces. No surfaces of higher order than two have been applied, such as an elliptical torus which is of fourth order. The reason for that is, that for each collision event of a neutron or a photon in a given cell the distances of this point to all surrounding surfaces have to be calculated. This is a rather long procedure in

the case of fourth order surfaces. Yet, the four conical surfaces do model the outer structures rather realistically. Fig.1 shows a fully 2π ASDEX Upgrade MCNP model in a vertical profile, from which the octant model AUG03 has been deduced. Also shown is the ASDEX Upgrade machine in a vertical profile. Fig.2 shows additionally several cuts of the octant model from different views. In addition to the tokamak machine also the concrete foundation, ceiling and walls are modeled. The wall has the form of a cylindrical shell with an inner radius of 12.0 meters, such that the air volume is identical with the real case.

2.2 Material Compositions, Masses of the Structures and Data Files

In chapter 2.1 the topology of the AUG03 model has been described. The next step is to input materials of different compositions to the single cells. In Tab.I all material data are listed for the tokamak structures. From the cell volumes and the specific densities the total masses of the structures are calculated. MCNP incorporates an elegant feature to calculate volumes of any asymmetric cell by ray tracing particles through a material-voided model. The particles start on a spherical sphere placed outside of the AUG03 model. The particle source is inward directed and cosine biased such that the model is isotropically flooded with particles. This method has been used to calculate the volumes of all cells of interest. In some cases (for example the stainless steel turnover structure ("Kippstruktur")) the densities have to be adjusted to meet the total amount of mass. This way of density "diluting" is a compromise; otherwise even a more detailed structuring of the model would be the consequence.

The MCNP-3A neutron data library consists mainly of ENDF/B-IV evaluations, including the Lawrence Livermore ENDL 85 files. A new data library on the basis of the first version of the European Fusion File EFF-1 has been added in 1989. This new file has been used in these calculations. The photon interaction tables are based on evaluated data from ENDF /2/ for all elements which are present in this AUG03 model.

2.3 Neutron Source Distributions

The toroidal neutron plasma source can be represented by the following analytical expression, see /3/:

$$S(a)=(1-(a/A)^2)^4 \quad 0 \leq a \leq A$$

with the normalized neutron source strength density $S(a)$. The parameter a defines the flux surface radius and runs from zero to the small plasma radius A . For noncylindrical plasmas the contour lines of constant strength density can be represented by

$$R=R_0 + a*\cos(t+D*\sin(t)) + e*(1-(a/A)^2)$$

$$z=E*a*\sin(t)$$

$$D=D_0*(a/A)$$

with $0 \leq a \leq A$ and the poloidal angle t ($0 \leq t < 2\pi$). Here R_0 and A are the large and the small plasma radii, respectively; E is the elongation, e the excentricity and D_0 the maximum triangularity. R is the radial distance to the tokamak centerline and z the poloidal distance to the midplane. This space dependant neutron source is added to MCNP in form of a Fortran subroutine.

As to the energy dependancy of the plasma neutrons the plasma temperature T and the fusion reaction type (d-d or d-t) are input parameters; the Doppler broadened neutron spectrum is then calculated in MCNP.

For these runs, yet, a neutron source which is distributed uniformly in space has been modeled. This simplification is a rather reasonable choice for the activation calculations of the structures, collimation and some shielding investigations. It may not be advisable to use this source distribution for estimating the response of the fission detector assembly.

2.4 Photon Source Distribution

Neutron activation occurs all over the different tokamak structures, and thus is the photon source distribution. Yet, it would be an inconvenient and uneffective way to model photon sources allover the different structures. A compromise is to combine the distributed photon source together to two sources, one which is located near the very center of the tokamak and one near the outer structures. The inner vacuum chamber wall has been chosen as the first one and represents all photon sources from the center parts (vacuum chamber wall and passive stabilizers). The outer position for the second photon source is located inside the toroidal field coil section, see fig.3. In this figure also the location of the volumetric neutron source is shown. The photon energy spectra differ for the isotopes under study. An average energy distribution should be formed combining all these isotope sources together. Here, for simplification a constant average photon energy of 1 MeV has been chosen.

As an example for MCNP input data, Appendix A lists the AUG03 input data file for neutron activation calculations. The input file consists mainly of four parts defining the cells, the surfaces enclosing those cells, the material compositions of cells and, finally the definition of the source and the tallies to be investigated. A tally is defined by the cell in which to calculate the flux. In addition with a multiplier card, defining the reaction path of an isotope and its isotope density, the specific reactions per source particle are tallied.

3. Neutron Activation Calculations

3.1 Structures, Isotopes and Activation Cross Sections

Five dominant tokamak structures and, in addition, the content of argon in the experimental hall have been chosen for activation calculations, see Tab.II. In this table the structures, neutron reactions with different isotopes, half lives of the products and the isotope densities are listed. Both, radiative (n, γ)-capture as well (n,p)-reactions have been investigated. The cross section tables of the isotopes are from different files, which are also included. Furthermore, these cross sections are shown in figs.4 to 8. For the isotope Fe-54 no (n,p)-cross sections have been available, so the (n,p)-cross section of the element Fe has been used. The energy dependant shapes are similar in form, yet the absolute values differ by a factor of about four to six /4/. This difference can be corrected by increasing the Fe-54 density artificially by a factor of five in the calculations. Unfortunately the Lawrence Livermore Dosimetry File LLL DOS is not yet implemented for display and graphics, so the cross section plot of Cu-63 (n, γ) can not be shown here.

3.2 Neutron Spectra from d-d and d-t Plasma Neutrons

Together with the neutron activation calculations also the energy dependant neutron fluxes have been tallied for the structures of interest. The amount of histories has been chosen to produce an statistical error in the group fluxes below 2%. This is achieved with about 10^5 histories per run.

In the following tables and figures relating to the neutron fluxes (n/cm²*sec) the normalization is always per 10^{16} source neutrons per second in the case of d-d neutrons, and per 10^{13} source neutrons per second in the d-t case. The tables list the group fluxes $\Phi(E)\Delta E$, neutron fluxes $\Phi(E)$ per MeV and the lethargy fluxes $\Phi(u)$ per lethargy interval. The neutron lethargy is defined as $u=-\ln(E)$. In the figures the fluxes $\Phi(E)$ and $\Phi(u)$ are plotted.

The neutron spectra in the stainless steel vacuum vessel and the air space of the experiment hall are shown: Figs. 9, 9a, 10 and 10a for the vacuum vessel and figs. 11, 11a, 12 and 12a for the air space of the experimental hall. In addition to these figures, the Tables III and IV list the data for the vacuum vessel, and tables V and VI for the air space, respectively.

The thermal fluxes inside the tokamak structures are rather small compared to the total ones. For example, the thermal flux portion in the vacuum vessel is less than 1.5% for

0.27%, at the turnover structure 0.3-0.9% depending on the location, at the toroidal field coils 5.5% and at the poloidal field coils about 10%. As to the air space the thermal flux amounts to 32% for d-d-neutrons and 26% for d-t-neutrons. From this one can already deduce that the neutron activation inside the tokamak structures will be due both to thermal and fast neutrons.

3.3 Neutron Activation and Activities

In contrary to neutron spectra evaluation, in the case of activation calculations only two energy groups have been tallied, one covering the thermal energy range and a second one from epithermal to MeV energies. The reason is because in the case of activation the energy dependence is of very little interest. AUG03 tallies the amount of activation for a given isotope in a cell per source neutron. Of further interest to this value is the amount of activations after a cycle of single plasma discharges. This cycle is defined as follows: 10 shots per 5 seconds with a constant neutron source strength of 10^{16} n/s; the time interval between the single shots is 10 minutes. The total activation after this specific discharge cycle can be calculated by paying regard to the decay during the cooling intervals. The activities (in Bq) are calculated for the end of the shot cycle. Table VII shows the results of activations. Listed are the activation data per source neutron, the total activation after this specific shot cycle and the resulting activities in Bq. The following row of Table VII lists the portion of activations due to thermal neutrons. Similar calculations have been performed with 14.7 MeV d-t-neutrons. The last row shows the ratios of activation of d-t-plasma neutrons to d-d-plasma neutrons.

The statistical errors of these activation data range in between 1% to 4%. One can see that the amount of activation due to thermal neutrons varies within a rather large range depending on the specific isotope and the location. The activation due to the 14.7 MeV d-t-neutrons, related to the same neutron source strength as the 2.5 MeV d-d-neutrons, is about 3% to 20% higher for radiative capture. Yet, in the case of the (n,p) threshold reactions the difference is rather large with a factor ranging from 35 to 55.

4. Photon Transport Calculations and Dose Rates

The photon portion of MCNP with the Detailed Physics Treatment has been used for photon transport calculations. The real photon source is distributed all over the tokamak machine. In these calculations two photon sources have been investigated as already mentioned in chapter 2.4. At three different locations the resulting photon fluxes are calculated: 1. the area of the vacuum chamber, 2. at a distance of 6 meters from the tokamak center and 3. near the concrete wall inside the experimental hall. The photon fluxes (number of photons/cm²*sec) are, as in the neutron transport case, tallied per source photon per second. Tab. VIII shows the results of these photon transport calculations. For all three loca-

tion the photon fluxes are listed for the two cases of photon sources. The fluxes at the two positions in the experimental hall differ by a factor of about 2.5 depending on the source location. For the vacuum area this difference amounts up to a factor of 50.

To account for the total photon fluxes after the specific shot cycle one has to sum up the isotope activities for the inner structures and outer structures separately and weigh them with the corresponding fluxes per source photon. This yields the total photon fluxes after the shot cycle. These results are shown in Tab. IX together with the photon dose rates in mSv/hr, by using the conversion factors as shown in Tab. X. The photon flux calculations have been performed energy dependantly and the results show that the average photon energy at all three locations is about a factor of 2 to 3 lower than the 1 MeV input energy which is mainly due to Compton effects. The conversion factor between photon flux and dose rate has been taken at 500 keV photon energy.

The (n,p) threshold reactions in Fe-54 and Ni-58 do not play an important role regarding the dose rates just after one specific shot cycle; yet, due to the long half live times of the products the accumulation of these activities may play some role if one considers long range tokamak operation times of months or years.

The activation of Argon-40, which leads to an unstable isotope of 1.83 hours half live time is mainly due to thermal neutrons. The resulting activity must be considered to assess radiation levels inside the tokamak experimental hall.

5. Summary and Conclusions

The Monte Carlo Code MCNP version 3A has been applied to model ASDEX Upgrade for neutron activation and photon transport problems. This code is versatile to account for both neutron and photon transport within the same topology of the tokamak model. The data libraries for both neutron and photon cross sections which have been used are up to date for both 2.5 MeV d-d-neutron and photon transport calculations. There may still exist some discrepancies for the 14.7 MeV d-t-neutron range. This energy range, however, is only of a marginal interest of range for this present case of activation calculations.

References:

- /1/ W. KÖPPENDÖRFER and the ASDEX UPGRADE TEAM, Completion of Assembly and Start of Technical Operation at ASDEX Upgrade, Proceedings 16th Symposium on Fusion Technology (SOFT), Sept. 1990, London, UK, to be published
- /2/ J. B. BRIESMEISTER, ed., "MCNP, A General Monte Carlo Code for Neutron and Photon Transport", Version 3A, LA-7396-M, Rev.2 Manual, Sept. 1986
- /3/ U. FISCHER, Die neutronenphysikalische Behandlung eines (d,t) Fusionsreaktors nach dem Tokamakprinzip (NET), Ph.D. Thesis University Karlsruhe, June 1990, KfK-4790 Report, Kernforschungszentrum Karlsruhe
- /4/ B. GOEL , Graphical Representation of the German Nuclear Data Library KEDAK, Part 1: Nonfissile Materials, KfK-2233 Report, NEANDC(E) 170 U, Dec. 1975
- /5/ L. P. KU, J. G. KOLIBAL, S. L. LIEW, A Comparison of 1-, 2-, and 3-dimensional Modeling of the TFTR for NUCLEAR Radiation Transport Analysis, PPPL-2244, Princeton University, Princeton, N.J., Sept. 1985

APPENDIX A

MCNP Input Data File for AUG03 Neutron Activation
Calculations

3D : ASDEX UPGRADE MODEL AUG03 (ACTIVATION CALCULATIONS)

```
C
C CCCCCCCCCCCCCCCCCC
C CELL CARDS C
C CCCCCCCCCCCCCCCCCC
C
C TOKAMAK MODELING
C =====
C CELL 5 CENTRAL COLUMN
5 1 -8.7 340 -490 -5 -607 610 940
C CELL 10 - CENTRAL POL. FIELD COIL
10 2 -8.0 340 -490 5 -10 -607 610 940
C CELL 20 INNER TOR. FIELD COIL
20 2 -5.3 340 -490 10 -20 -607 610
C CELL 30 INNER VACUUM CHAMBER WALL
30 3 -8.7 360 -470 20 -30 -607 610
C CELL 40 INNER GRAPHITE LINER
40 4 -1.85 370 -460 30 -40 -607 610
C CELL 50 UPPER HORIZ. VACUUM CHAMBER WALL INCL. DIVERTOR
50 3 -8.7 460 -470 30 -220 -607 610
C CELL 60 LOWER "
60 3 -8.7 360 -370 30 -270 -607 610
C CELL 70 UPPER CONICAL VACUUM CHAMBER WALL
70 3 -8.7 -460 210 -220 430 -607 610
C CELL 80 LOWER "
80 3 -8.7 370 260 -270 -410 -607 610
C CELL 90 PORTWINDOW
90 3 -8.7 125 -130 410 -430 -607 610
C CELL 100 UPPER GRAPHITE LINER
100 4 -1.85 455 -460 40 -210 -607 610
C CELL 110 LOWER "
110 4 -1.85 370 -380 40 -260 -607 610
C CELL 120 VACUUM CHAMBER WALL OUTSIDE
120 3 -8.7 410 -430 80 -90 610 -604 940
C CELL 130 "
130 3 -8.7 410 -430 80 -90 605 -607 940
C
C PLASMA REGION
C =====
C CELL 150 VACUUM VOLUME WITHOUT SOURCE REGION
150 0 40 380 -455 (-210;-430) -80 (410;-260) -607 610 #151 #152
#153 #154 #155
C CELL 151 SOURCE REGION
151 0 700 703 -702 -704 -701 -705 -607 610 940
C
C PASSIVE STABILIZERS
C =====
C UPPER STABILIZER
152 15 -8.8 1104 -1105 1102 -1103 -607 610
C GRAPHITE LINER
153 4 -1.85 1104 -1105 1101 -1102 -607 610
C LOWER STABILIZER
154 15 -8.8 1114 -1115 1112 -1113 -607 610
C GRAPHITE LINER
155 4 -1.85 1114 -1115 1111 -1112 -607 610
C
C STUETZSTRUKTUR
C =====
C CELLS 160 TO 164 UPPER HORIZONTAL STRUCTURE
160 7 -4.85 510 -520 160 -170 -607 610 940
161 7 -4.85 510 -520 20 -160 606 -607 990
162 7 -4.85 510 -520 20 -160 608 -609 940
163 7 -4.85 510 -520 20 -160 610 -611 -990
164 7 -4.85 490 -520 -20 -607 610 940
C CELLS 170 TO 174 LOWER HORIZONTAL STRUCTURE
170 7 -4.85 310 -320 160 -170 -607 610 940
171 7 -4.85 310 -320 20 -160 606 -607 990
172 7 -4.85 310 -320 20 -160 608 -609 940
```


173 7 -4.85 310 -320 20 -160 610 -611 -990
174 7 -4.85 310 -340 -20 -607 610 940
C CELLS 181 TO 183 VERTICAL OUTER STRUCTURE
181 7 -4.85 320 -510 160 -170 606 -607 990
182 7 -4.85 320 -510 160 -170 608 -609 940
183 7 -4.85 320 -510 160 -170 610 -611 -990
C
C AIR SPACE IN BETWEEN STUETZSTRUKTUR
C =====
C CELLS 165 -166 UPPER
165 9 -0.0013 510 -520 20 -160 609 -606
166 9 -0.0013 510 -520 20 -160 611 -608
C CELLS 175 -176 LOWER
175 9 -0.0013 310 -320 20 -160 609 -606
176 9 -0.0013 310 -320 20 -160 611 -608
C CELLS 184 -185 OUTSIDE
184 9 -0.0013 320 -510 160 -170 609 -606
185 9 -0.0013 320 -510 160 -170 611 -608
C
C POLOIDAL FIELD COILS
C =====
C CELL 190 UPPER POL. COIL #1
190 8 -6.51 500 -510 50 -60 -607 610 940
C CELL 200 LOWER POL. COIL #2
200 8 -6.51 320 -330 50 -60 -607 610 940
C CELL 210 AIR SPACE AROUND UPPER COIL #1
210 9 -0.0013 490 -510 20 -160 -607 610 940 #190
C CELL 220 AIR SPACE AROUND LOWER COIL #2
220 9 -0.0013 320 -340 20 -160 -607 610 940 #200
C CELL 230 POL. COIL #3
230 8 -6.51 480 -490 100 -120 -607 610 940
C CELL 240 POL. COIL #4
240 8 -6.51 340 -350 100 -120 -607 610 940
C CELL 250 AIR SPACE AROUND #3
250 9 -0.0013 450 -490 240 -160 -607 610 940 #230
C CELL 260 AIR SPACE AROUND #4
260 9 -0.0013 340 -390 290 -160 -607 610 940 #240
C
C TOROIDAL FIELD COILS
C =====
C CELLS 271 TO 273 UPPER HORIZONTAL PARTS
271 10 -5.30 470 -490 20 -240 606 -607 990
272 10 -5.30 470 -490 20 -240 608 -609 940
273 10 -5.30 470 -490 20 -240 610 -611 -990
C CELLS 281 TO 283 LOWER "
281 10 -5.30 340 -360 20 -290 606 -607 990
282 10 -5.30 340 -360 20 -290 608 -609 940
283 10 -5.30 340 -360 20 -290 610 -611 -990
C CELLS 291 TO 293 UPPER CONICAL PARTS
291 10 -5.30 -470 -230 220 -240 606 -607 990 430
292 10 -5.30 -470 -230 220 -240 608 -609 940 430
293 10 -5.30 -470 -230 220 -240 610 -611 -990 430
C CELLS 301 TO 303 LOWER "
301 10 -5.30 360 -280 270 -290 606 -607 990 -410
302 10 -5.30 360 -280 270 -290 608 -609 940 -410
303 10 -5.30 360 -280 270 -290 610 -611 -990 -410
C CELLS 311 TO 313 OUTER CYLINDR. "
311 10 -5.30 410 -430 90 -125 606 -607 990
312 10 -5.30 410 -430 90 -125 608 -609 940
313 10 -5.30 410 -430 90 -125 610 -611 -990
C
C KIPPSTRUKTUR
C =====
C CELLS 274 TO 275 BETWEEN UPPER HORIZ. FIELD COILS
274 12 -4.8 470 -490 20 -240 609 -606 940
275 12 -4.8 470 -490 20 -240 611 -608 940
C CELLS 284 TO 285 BETWEEN LOWER "
284 12 -4.8 340 -360 20 -290 609 -606 940

285 12 -4.8 340 -360 20 -290 611 -608 940
C CELLS 294 TO 295 BETWEEN UPPER CONICAL FIELD COILS
294 12 -4.8 -470 -230 220 -240 609 -606 940 430 #296
295 12 -4.8 -470 -230 220 -240 611 -608 940 430 #297
C CELLS 304 TO 305 BETWEEN LOWER " "
304 12 -4.8 360 -280 270 -290 609 -606 940 -410 #306
305 12 -4.8 360 -280 270 -290 611 -608 940 -410 #307
C
C CYLINDERS IN KIPPSTRUKTUR ABOVE AND BELOW BOTH PORTS
C =====
C LARGE PORT WINDOW
C CELL 296 UPPER CYLINDER
296 0 -1230 220 -241 940
C CELL 297 LOWER CYLINDER
306 0 -1240 270 -291 940
C SMALL PORT WINDOW
C CELL 306 UPPER CYLINDER
297 0 -1210 220 -241 940
C CELL 306 LOWER CYLINDER
307 0 -1220 270 -291 940
C
C PORTS
C =====
C CELLS 314 AND 315 ARE THE SMALL AND LARGE PORT AREA
C LARGE PORT
314 0 410 -430 80 -125 604 -605 940
C KIPPSTRUKTUR AROUND LARGE PORT
315 12 -4.8 410 -430 90 -125 605 -606 940
316 12 -4.8 410 -430 90 -125 609 -604 940
C SMALL PORT
317 0 90 -125 -1200 940
C KIPPSTRUKTUR AROUND SMALL PORT
318 12 -4.8 410 -430 90 -125 611 -608 #317
C
C POLOIDAL FIELD COILS #5 AND #6
C =====
C CELL 320 POLOIDAL COIL #5
320 8 -6.51 440 -450 140 -150 -607 610 940
C CELL 330 POLOIDAL COIL #6
330 8 -6.51 390 -400 140 -150 -607 610 940
C CELL 325 AIR SPACE AROUND #5
325 9 -0.0013 430 -450 230 -160 -607 610 940 #320
C CELL 335 AIR SPACE AROUND #6
335 9 -0.0013 390 -410 280 -160 -607 610 940 #330
C CELL 340 AIR SPACE BEFORE THE PORTS
340 9 -0.0013 410 -430 130 -160 -607 610 940
C
C REGION UNDER THE TOKAMAK
C =====
C CELL 350 SUPPORTING PILLARS (HOMOGENIZED)
350 7 -2.10 300 -310 170 -180 -607 610 940
C CELL 360 AIR SPACE
360 9 -0.0013 300 -310 -170 -607 610 940
C
C TOKAMAKHALL AND WALLS
C =====
C CELL 400 TOTAL AIR SPACE IN EXP. HALL
400 9 -0.0013 300 -810 -190 (170:520) -607 610 940
#350 #360
C CELL 410 CONCRETE FLOOR
410 11 -2.25 800 -300 -195 -607 610 940
C CELL 420 CONCRETE CEILING
420 11 -2.25 810 -820 -195 -607 610 940
C CELL 430 CONCRETE WALL
430 11 -2.25 300 -810 190 -195 -607 610 940
C
C
C OUTSIDE WORLD

```
C          =====
5000 0    -800:195:607:-610:820:-940
C

C          CCCCCCCCCCCCCCCCCCCC
C          SURFACE CARDS      C
C          CCCCCCCCCCCCCCCCCCCC
C
C
C          TOKAMAKSTRUCTURES
C          =====
C          PLANES VERTICAL TO Z-AXIS
300 PZ -540
310 PZ -308
320 PZ -260
330 PZ -214
340 PZ -190
350 PZ -145.5
360 PZ -145
370 PZ -137.8
380 PZ -135.6
390 PZ -83.033089
400 PZ -54
410 PZ -40
C 420 PZ 0 NOT USED
430 PZ 40
440 PZ 54
450 PZ 83.033089
455 PZ 135.6
460 PZ 137.8
470 PZ 145
480 PZ 145.5
490 PZ 190
500 PZ 214
510 PZ 260
520 PZ 308
300 PZ -680
310 PZ 1180
820 PZ 1380
C
C          PLANE VERTICAL TO Y-AXIS
C          PLANE 940 IS AMBUIGITY SURFACE TO DEFINE THE OCTANT
940 PY 0
C
C          PLANE VERTICAL TO X-AXIS
C          PLANE 990 IS AMBUIGITY SURFACE TO DEFINE THE OCTANT
990 PX 0
C
C          OTHER PLANES
604 P 9.8963 -1 0 0
605 P 3.3268 -1 0 0
606 P 2.4142 -1 0 -47.036
C          PLANES 607 AND 610 ARE REFLECTING PLANES
*607 P 2.4142 -1 0 0
608 PX -18
609 PX 18
*610 P 2.4142 1 0 0
611 P 2.4142 1 0 47.036
C
C          CYLINDERS PARALLEL TO Z-AXIS
5 CZ 25
10 CZ 51
20 CZ 92.4
30 CZ 96
40 CZ 96.5
50 CZ 126
60 CZ 206
80 CZ 272
```

90 CZ 276
100 CZ 292
120 CZ 337
125 CZ 335
130 CZ 337
140 CZ 346
150 CZ 374
160 CZ 381
170 CZ 425
180 CZ 480
190 CZ 1198
195 CZ 1300

C
C COMMON CYLINDER FOR SMALL PORT
1200 GQ 0.962 0.03806 1 0.38268 0 0 0 0 0 -200

C
C CONI PARALLEL TO Z-AXIS
210 KZ 326.57 .8763 -1
220 KZ 330 .8763 -1
230 KZ 951.7 .1366 -1
240 KZ 426 .8763 -1
260 KZ -326.57 .8763 1
270 KZ -330 .8763 1
280 KZ -951.7 .1366 1
290 KZ -426 .8763 1

C
C SURFACES FOR SOURCE CELL
700 CZ 100.0
701 CZ 150
702 PZ 60
703 PZ -60
704 KZ 188 .8763 -1
705 KZ -188 .8763 1

C
C SURFACES FOR STABILIZERS AND GRAPHITE
1114 PZ -89
1115 PZ -54
1104 PZ 54
1105 PZ 89
1101 KZ 365.9 .4473 -1
1102 KZ 368.5 .4473 -1
1103 KZ 382.7 .4473 -1
1111 KZ -365.9 .4473 1
1112 KZ -368.5 .4473 1
1113 KZ -382.7 .4473 1

C
C CYLINDERS FOR TUBES ABOVE AND BELOW THE PORTS
1210 GQ 0.962 0.03806 1 0.38268 0 0 0 0 -202 10032.
1220 GQ 0.962 0.03806 1 0.38268 0 0 0 0 202 10032.
1230 GQ 0.962 0.03806 1 -0.38268 0 0 0 0 -202 10032.
1240 GQ 0.962 0.03806 1 -0.38268 0 0 0 0 202 10032.
241 KZ 424.0 0.8763 -1
291 KZ -424.0 0.8763 1

C
C
C CCCCCCCCCCCCCCCCCC
C MATERIAL CARDS C
C CCCCCCCCCCCCCCCCCC

C FE CR MN
M1 26000.89C -0.6495 24000.89C -0.1750 25055.89C -0.018
C NI CU MO
28000.89C -0.1225 29000.89C -0.01 42000.89C -0.025

C

```
C      CU              SI              C
M2    29000.89C -0.961 14000.89C -0.0028 6000.89C -0.0207
C      H              O
      1001.89C -0.0021 8016.89C -0.0134
-----
C      FE              CR              MN              NI
M3    26000.89C -0.705 24000.89C -0.183 25055.89C -0.012 28000.89C -.10
C
C
M4    6000.89C 1.0
-----
C      FE              CR              NI
M7    26000.89C -.716 24000.89C -.181 28000.89C -.091
C      MN
      25055.89C -.012
-----
C      CU              H              O              SI
M8    29000.89C -.937 1001.89C -0.004 8016.89C -0.032 14000.89C -.027
C
C      O              N
M9    8016.89C -0.22 7014.89C -0.78
-----
C      CU              SI              C
M10   29000.89C -0.961 14000.89C -.0028 6000.89C -.0207
C      H              O
      1001.89C -0.0021 8016.89C -0.0134
-----
C      H              O              MA              MG
M11   1001.89C -0.0045 8016.89C -0.51 11023.89C -0.011 12000.89C -.004
C      AL              SI              K              CA
      13027.89C -0.035 14000.89C -.36 19000.89C -.014 20000.89C -.0455
C      FE
      26000.89C -.016
-----
C      FE              CR              MN
M12   26000.89C -0.663 24000.89C -0.184 25055.89C -0.0816
C      NI
      28000.89C -0.0714
-----
C
C      CU
M15   29000.89C 1.0
-----
C
C
C
C
C
C      MATERIALS FOR TALLY-MULTIPLIERS:
C      ++++++
C      ARGON
M999  18000.01C 1.0
C
C      MANGAN 55
M998  25055.89C 1.0
C
C      CHROMIUM 50
M997  24050.30Y 1.0
C
C      COPPER 63
M996  29063.30Y 1.0
C
C      NICKEL 58
M994  28058.35C 1.0
C
C      IRON 58 (HERE:ELEMENT IRON !)
M995  26000.89C 1.0
C
C
```

```
C =====
C
C
MODE N
C SOURCE IN CELL 151
SDEF POS=0 0 0 CEL=151 RAD=D2 ERG=D1
EXT=D3 AXS= 0 0 1
SI2 100 150
SI3 60
SP1 -4 -0.001 -1
C D-D NEUTRON SOURCE IN CELL 151 T=1 KEV
C
IMP:N 1 89R 0
C
C CCCCCCCCCCCCCCCCCC
C TALLY CARDS C
C CCCCCCCCCCCCCCCCCC
C VOLUMES SET TO ONE
VOL 1 89R 0
C
C ENERGY GROUPS
C
E0 1.E-11 4.1399E-07 3.9279E-6 3.7267E-05 3.5358E-04 3.3546E-03
3.1828E-02 1.6573E-01 3.0197E-01 5.5023E-01 6.7206E-01
8.2085E-01 1.0026 1.2246 1.6530 2.2313 2.7253 3.6788 4.9659
6.7032 8.1873 10 11.052 12.214 13.499 14.918
C
C CELL FLUXES
C =====
C (ACTIVATION)
C
C
F4:N 165 184 325 340 360 400
FC4 ARGONACTIVATION IN THE HALL
C MULTIPLIER CARD
C ATOMDENSITY MATERIAL REAKTIONSPATH
FM4 1.385E-07 999 102
C
F14:N 30 50 70 120 130
FC14 MANGANACTIVATION VACUUM CHAMBER WALL
C MULTIPLIER CARD
FM14 1.14E-03 998 102
C
F24:N 30 50 70 120 130
FC24 CHROMIUMACTIVATION VACUUM CHAMBER WALL
C MULTIPLIER CARD
FM24 8.30E-04 997 102
C
F34:N 190 230 320
FC34 KOPPER 63 ACTIVATION POL. COILS
C MULTIPLIER CARD
FM34 3.08E-02 996 102
C
F44:N 152
FC44 COPPER 63 ACTIVATION OF THE PASSIVE STABILIZERS
C MULTIPLIER CARD
FM44 5.790E-02 996 102
C
F54:N 272 292 312
FC54 COPPER 63 ACTIVATION TF-COIL OUTSIDE
C MULTIPLIER CARD
FM54 3.230E-02 996 102
C
F64:N 20
FC64 COPPER 63 ACTIVATION TF-COIL INSIDE
C MULTIPLIER CARD
FM64 3.230E-02 996 102
C
```

FC74 MANGANACTIVATION KIPPSTRUKTUR
C MULTIPLIER CARD
FM74 4.27E-03 998 102
C
F84:N 274 294
FC84 CHROMIUMACTIVATION KIPPSTRUKTUR
FM84 4.61E-04 997 102
C
C REACTION FE(N,P)
C
F164:N 30 50 70 120 130
FC164 FE(N,P) IN THE VACUUM CHAMBER WALL
C MULTIPLIER CARD
FM164 6.52E-02 995 103
C
F174:N 274 294
FC174 FE(N,P) IN THE KIPPSTRUKTUR
C MULTIPLIER CARD
FM174 3.41E-02 995 103
C
C REACTION NI-58 (N,P)
C
F184:N 30 50 70 120 130
FC184 NI-58 (N,P) REAKTION IN THE VACUUM CHAMBER WALL
C MULTIPLIER CARD
FM184 6.12E-03 994 103
C
F194:N 274 294
FC194 NI-58 (N,P) REACTION IN THE KIPPSTRUKTUR
C MULTIPLIERCARD
FM194 2.41E-03 994 103
C
C CC
C CUT NEUTRON ENERGY RANGE
CUT:N 1J 1.0E-11 0.0 0.0
PRINT
CTME 0.30
NPS 1000000

Tab.I Composition of Materials and Masses
(Weight %)

1.	Vacuum Vessel:	Fe	70.6	
		Cr	18.2	
		Ni	10.0	
		Mn	1.2	Total Mass: 29600 kg
2.	Passive Stabilizers:	Cu	100.0	Total Mass: 7500 kg
3.	Toroidal Field Coils:	Cu	96.1	
		Si	0.28	
		C	2.07	
		H	0.21	
		O	1.34	Total Mass: 9375 kg (one Coil)
4.	Turnover Structure: "Kippstruktur"	Fe	66.3	
		Cr	18.4	
		Mn	8.16	
		Ni	7.14	Total Mass: 130000 kg
5.	Poloidal Field Coils:	Cu	93.33	
		C	3.09	
		H	0.43	
		O	2.54	
		Si	0.60	Total Mass: 125000 kg
6.	PF-Structure "Stützstruktur"	Fe	71.6	
		Cr	18.1	
		Ni	9.1	
		Mn	1.2	Total Mass: 195000 kg
7:	Graphite:	C	100	
				Inner Wall: 150 kg
				Divertors : 566 kg
				Stabilizers: 290 kg
				Total Mass: 1006 kg
8.	Concrete:	H	0.45	
		O	51.0	
		Na	1.1	
		Mg	0.4	
		Al	3.5	
		Si	36.0	
		K	1.4	
		Ca	4.5	
		Fe	1.6	

Tab. II ASDEX-Upgrade Structures and Neutron Reaction Paths which have been investigated in these Calculations

Isotopes	Reaction Path	Half Live $T_{1/2}$	Isotope Density (atom/barn*cm)
Vacuum Chamber Wall			
Cr-50	(n,Gamma)	27.7 d	7.95E-04
Fe-54	(n,p)	312.2 d	3.80E-03
Mn-55	(n,Gamma)	2.58 h	1.14E-03
Ni-58	(n,p)	70.8 d	6.05E-03
Passive Stabilizers			
Cu-63	(n,Gamma)	12.7 h	5.74E-02
Toroidal Field Coils			
Cu-63	(n,Gamma)	12.7 h	3.33E-02
Poloidal Field Coils			
Cu-63	(n,Gamma)	12.7 h	3.98E-02
"Kippstruktur"			
Cr-50	(n,Gamma)	27.7 d	4.43E-04
Fe-54	(n,p)	312.2 d	1.98E-03
Mn-55	(n,Gamma)	2.58 h	4.28E-03
Ni-58	(n,p)	70.8 d	2.38E-03
Air Space of Exp. Hall			
Ar-40	(n,Gamma)	1.83 h	1.38E-07

Tab.III Spectral Neutron Fluxes at the Vacuum Vessel for 2.45 MeV
d-d-Source Neutrons at ASDEX-Upgrade
Normalization is per 1.0E+16 Neutrons per Second

Energies (MeV)		Spectral Neutron Fluxes		
Lower	Upper	(n/cm ² *s)	(n/cm ² *s*MeV)	per lethargy Interval
1.000E-11	4.140E-07	3.995E+08	9.651E+14	3.758E+07
4.140E-07	3.930E-06	1.803E+09	5.127E+14	8.010E+08
3.930E-06	3.730E-05	4.033E+09	1.209E+14	1.792E+09
3.730E-05	3.540E-04	5.414E+09	1.710E+13	2.406E+09
3.540E-04	3.350E-03	8.292E+09	2.768E+12	3.690E+09
3.350E-03	3.180E-02	1.121E+10	3.940E+11	4.980E+09
3.180E-02	1.660E-01	1.670E+10	1.244E+11	1.010E+10
1.660E-01	3.020E-01	9.510E+09	6.993E+10	1.589E+10
3.020E-01	5.500E-01	1.208E+10	4.871E+10	2.015E+10
5.500E-01	6.720E-01	4.895E+09	4.012E+10	2.443E+10
6.720E-01	8.210E-01	3.909E+09	2.623E+10	1.952E+10
8.210E-01	1.003E+00	4.201E+09	2.313E+10	2.102E+10
1.003E+00	1.225E+00	3.518E+09	1.582E+10	1.756E+10
1.225E+00	1.653E+00	6.815E+09	1.592E+10	2.274E+10
1.653E+00	2.231E+00	3.828E+09	6.623E+09	1.277E+10
2.231E+00	2.725E+00	1.213E+10	2.456E+10	6.065E+10

Total=1.087E+11

Tab.IV Spectral Neutron Fluxes at the Vacuum Vessel for 14.7 MeV
d-t-Source Neutrons at ASDEX-Upgrade
Normalization is per 1.0E+13 Neutrons per Second

Energies (MeV)		Spectral Neutron Fluxes		
Lower	Upper	(n/cm ² *s)	(n/cm ² *s*MeV)	per lethargy Interval
1.000E-11	4.140E-07	7.66E+05	1.85E+12	7.21E+04
4.140E-07	3.930E-06	3.62E+06	1.03E+12	1.61E+06
3.930E-06	3.730E-05	8.79E+06	2.63E+11	3.91E+06
3.730E-05	3.540E-04	1.20E+07	3.80E+10	5.35E+06
3.540E-04	3.350E-03	1.88E+07	6.28E+09	8.37E+06
3.350E-03	3.180E-02	2.56E+07	9.00E+08	1.14E+07
3.180E-02	1.660E-01	3.88E+07	2.89E+08	2.35E+07
1.660E-01	3.020E-01	2.26E+07	1.66E+08	3.77E+07
3.020E-01	5.500E-01	2.74E+07	1.10E+08	4.56E+07
5.500E-01	6.720E-01	1.02E+07	8.38E+07	5.11E+07
6.720E-01	8.210E-01	8.23E+06	5.52E+07	4.11E+07
8.210E-01	1.003E+00	7.19E+06	3.96E+07	3.60E+07
1.003E+00	1.225E+00	6.55E+06	2.94E+07	3.27E+07
1.225E+00	1.653E+00	6.89E+06	1.61E+07	2.30E+07
1.653E+00	2.231E+00	5.00E+06	8.64E+06	1.67E+07
2.231E+00	2.725E+00	2.52E+06	5.10E+06	1.26E+07
2.725E+00	3.679E+00	2.60E+06	2.73E+06	8.67E+06
3.679E+00	4.966E+00	1.59E+06	1.24E+06	5.31E+06
4.966E+00	6.703E+00	1.29E+06	7.44E+05	4.31E+06
6.703E+00	8.187E+00	1.01E+06	6.81E+05	5.05E+06
8.187E+00	1.000E+01	1.22E+06	6.73E+05	6.10E+06
1.000E+01	1.105E+01	4.91E+05	4.67E+05	4.91E+06
1.105E+01	1.221E+01	4.23E+05	3.64E+05	4.24E+06
1.221E+01	1.350E+01	1.52E+06	1.18E+06	1.52E+07
1.350E+01	1.492E+01	1.47E+07	1.04E+07	1.47E+08
		Total=2.30E+08		

Tab.V Spectral Neutron Fluxes in the Tokamak Hall for 2.45 MeV
d-d-Source Neutrons at ASDEX-Upgrade
Normalization is per 1.0E+16 Neutrons per Second
Fluxes are averaged over the whole Hall Volume

Energies (MeV)		Spectral Neutron Fluxes		
Lower	Upper	(n/cm ² *s)	(n/cm ² *s*MeV)	per Lethargy Interval
1.000E-11	4.140E-07	1.498E+08	3.619E+14	1.409E+07
4.140E-07	3.930E-06	3.471E+07	9.872E+12	1.542E+07
3.930E-06	3.730E-05	4.291E+07	1.286E+12	1.907E+07
3.730E-05	3.540E-04	4.834E+07	1.526E+11	2.148E+07
3.540E-04	3.350E-03	4.983E+07	1.663E+10	2.217E+07
3.350E-03	3.180E-02	5.967E+07	2.097E+09	2.651E+07
3.180E-02	1.660E-01	7.169E+07	5.342E+08	4.338E+07
1.660E-01	3.020E-01	3.388E+07	2.491E+08	5.661E+07
3.020E-01	5.500E-01	2.755E+07	1.111E+08	4.595E+07
5.500E-01	6.720E-01	1.040E+07	8.527E+07	5.193E+07
6.720E-01	8.210E-01	8.436E+06	5.662E+07	4.213E+07
8.210E-01	1.003E+00	6.422E+06	3.537E+07	3.214E+07
1.003E+00	1.225E+00	5.586E+06	2.512E+07	2.788E+07
1.225E+00	1.653E+00	8.517E+06	1.990E+07	2.842E+07
1.653E+00	2.231E+00	7.906E+06	1.368E+07	2.637E+07
2.231E+00	2.725E+00	1.568E+07	3.173E+07	7.837E+07

Total=5.81E+08

Tab.VI Spectral Neutron Fluxes in the Tokamak Hall for 14.7 MeV
d-t-Source Neutrons at ASDEX-Upgrade
Normalization is per 1.0E+13 Neutrons per Second
Fluxes are averaged over the whole Hall Volume

Energies (MeV)		Spectral Neutron Fluxes		
Lower	Upper	(n/cm ² *s)	(n/cm ² *s*MeV)	per lethargy Interval
1.000E-11	4.140E-07	1.65E+05	3.98E+11	1.55E+04
4.140E-07	3.930E-06	4.14E+04	1.18E+10	1.84E+04
3.930E-06	3.730E-05	4.59E+04	1.37E+09	2.04E+04
3.730E-05	3.540E-04	5.15E+04	1.62E+08	2.29E+04
3.540E-04	3.350E-03	5.84E+04	1.95E+07	2.60E+04
3.350E-03	3.180E-02	7.41E+04	2.61E+06	3.29E+04
3.180E-02	1.660E-01	8.28E+04	6.17E+05	5.01E+04
1.660E-01	3.020E-01	4.13E+04	3.03E+05	6.89E+04
3.020E-01	5.500E-01	3.37E+04	1.36E+05	5.62E+04
5.500E-01	6.720E-01	1.21E+04	9.93E+04	6.05E+04
6.720E-01	8.210E-01	8.60E+03	5.77E+04	4.29E+04
8.210E-01	1.003E+00	6.83E+03	3.76E+04	3.42E+04
1.003E+00	1.225E+00	5.03E+03	2.26E+04	2.51E+04
1.225E+00	1.653E+00	4.65E+03	1.09E+04	1.55E+04
1.653E+00	2.231E+00	3.96E+03	6.85E+03	1.32E+04
2.231E+00	2.725E+00	2.53E+03	5.13E+03	1.27E+04
2.725E+00	3.679E+00	1.93E+03	2.02E+03	6.41E+03
3.679E+00	4.966E+00	1.57E+03	1.22E+03	5.22E+03
4.966E+00	6.703E+00	1.50E+03	8.61E+02	4.99E+03
6.703E+00	8.187E+00	5.40E+02	3.64E+02	2.70E+03
8.187E+00	1.000E+01	6.72E+02	3.71E+02	3.36E+03
1.000E+01	1.105E+01	6.51E+02	6.19E+02	6.51E+03
1.105E+01	1.221E+01	5.76E+02	4.96E+02	5.76E+03
1.221E+01	1.350E+01	8.46E+02	6.59E+02	8.46E+03
1.350E+01	1.492E+01	1.65E+04	1.16E+04	1.65E+05
		Total=6.62E+05		

Tab. VII Neutron Activation of the Isotopes in the
Different Structures

Isotope	Activation per Source Neutron	Total Acti- vation after Shot Cycle	Activity (Bq)	Thermal Activation (%)	(d,t) to (d,d) Activation *)
Vacuum Chamber Wall					
Cr-50	3.23E-03	1.62E+15	4.68E+08	23-35	1.08
Fe-54	2.37E-04	1.18E+14	3.05E+06	0	35.2
Mn-55	8.25E-03	4.04E+15	1.26E+10	10-15	1.13
Ni-58	2.61E-03	1.31E+15	1.47E+08	0	45.0
Passive Stabilizers					
Cu-63	6.12E-02	3.06E+16	4.65E+11	2.7	1.09
Toroidal Field Coils					
Cu-63	6.93E-01	3.47E+17	5.27E+12	30-35	1.17
Poloidal Field Coils					
Cu-63	3.16E-02	1.58E+16	2.40E+11	50-60	1.21
"Kippstruktur"					
Cr-50	4.55E-03	2.28E+15	6.60E+08	13-20	1.03
Fe-54	9.05E-05	4.53E+13	1.16E+06	0	43.7
Mn-55	6.16E-02	3.02E+16	9.39E+10	10-18	1.06
Ni-58	8.68E-04	4.34E+14	4.90E+07	0	55.0
Air Space of Exp. Hall					
Ar-40	8.47E-06	4.12E+12	4.33E+08	93	1.05

*) Related to the same neutron source strength

Tab. IX Dose Rates due to Photon Fluxes
at the three Positions

Position	Total Photon Flux after Shot Cycle (1/cm ² *s)	Dose (mSv/hr)
Plasmavolume	5.68E+06	52.0
6m from Tokamak- Center	1.53E+05	1.39
12m from Tokamak- Center	6.12E+04	0.56

Tab. X Photon Flux-to-Dose Rate Conversion
Factors /2/ (ICRP-21)

Photon Energy MeV	DF(E) (rem/hr) (photons/cm ² *s)
0.01	2.78E-06
0.015	1.11E-06
0.02	5.88E-07
0.03	2.56E-07
0.04	1.56E-07
0.05	1.20E-07
0.06	1.11E-07
0.08	1.20E-07
0.1	1.47E-07
0.15	2.38E-07
0.2	3.34E-07
0.3	5.56E-07
0.4	7.69E-07
0.5	9.09E-07
0.6	1.14E-06
0.8	1.47E-06
1.	1.79E-06
1.5	2.44E-06
2.	3.03E-06
3.	4.00E-06
4.	4.76E-06
5.	5.56E-06
6.	6.25E-06
8.	7.69E-06
10.	9.09E-06

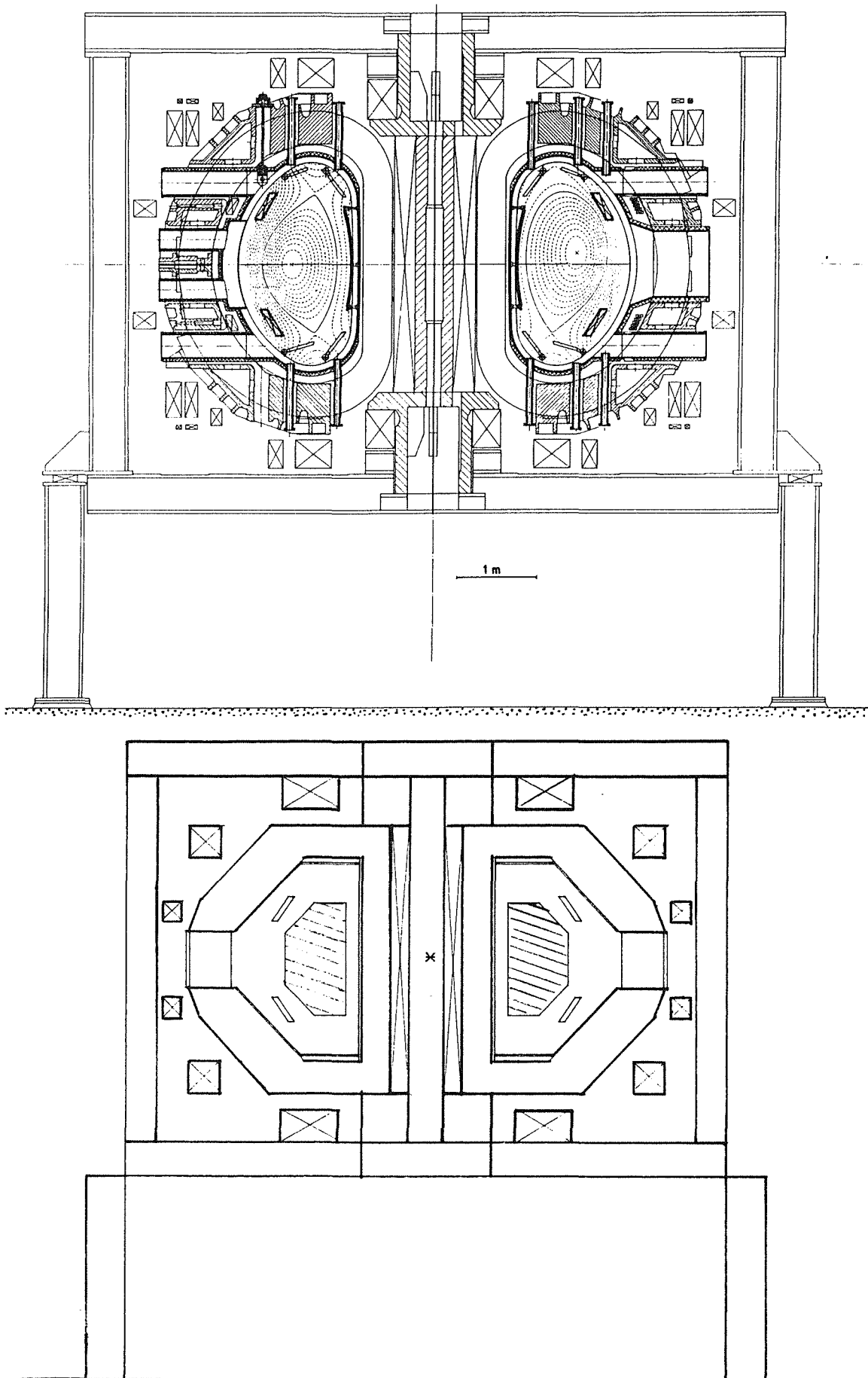


Fig.1 Vertical Cuts of the ASDEX-Upgrade Tokamak
and the Homogenized MCNP Model AUG01

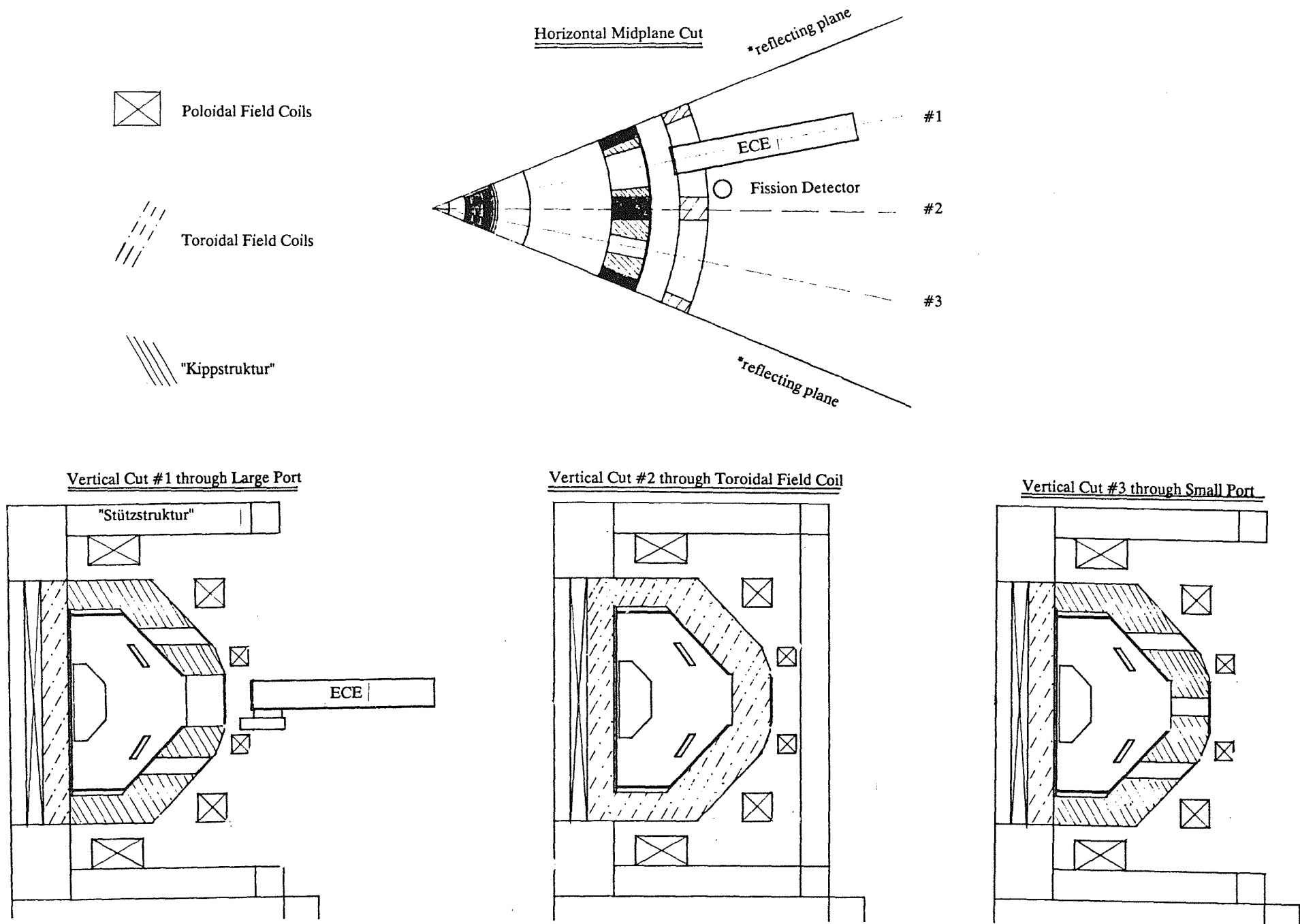


Fig.2 Graphs of the AUG03 Octant Model from Different Views

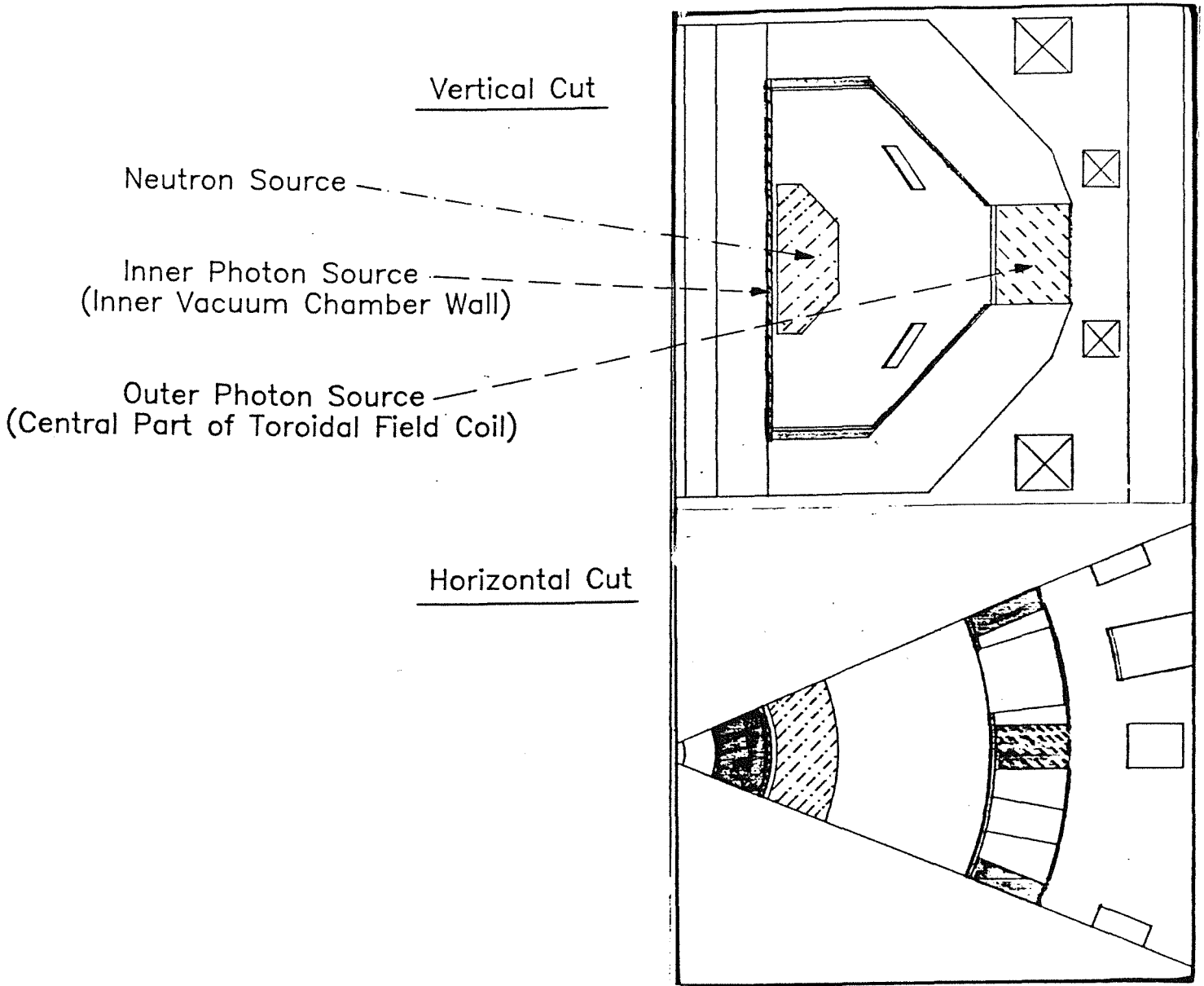


Fig.3 Locations of Volumetric Neutron and Photon Sources

CHROMIUM 50 (N,GAMMA) EFF1LIB REV1

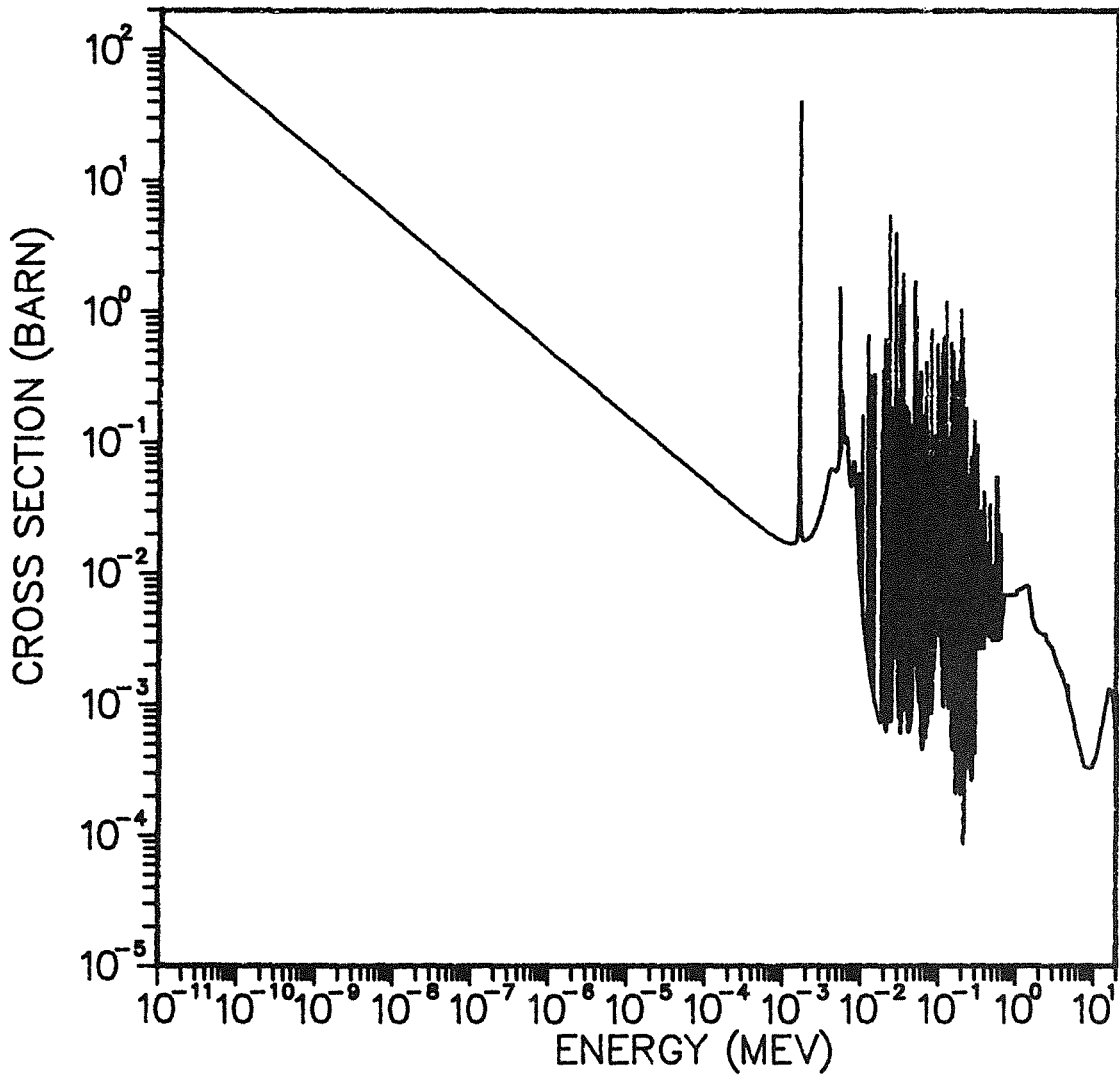


Fig. 4 Radiative Capture Cross Section of Chromium-50

PL07 1 09.16.38 TUES 16 OCT, 1980 JOB-INVO99 , REAFORCHARGEXENTRUM KWLSLWAVE DISPLAY 10.0

Mangan 55 (N,GAMMA) EFF1LIB REV1

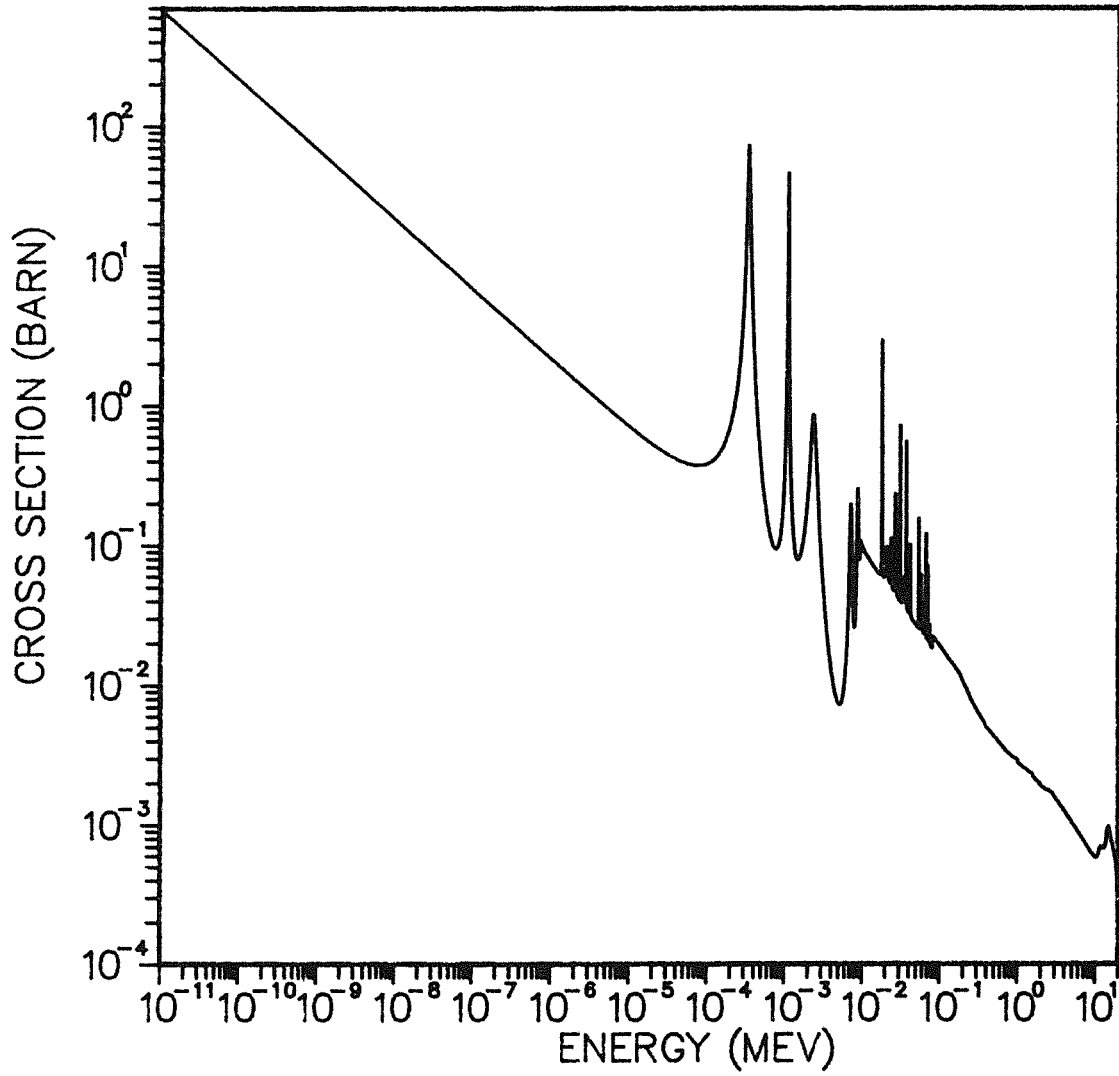


Fig. 5 Radiative Capture Cross Section of Manganin-55

IRON (N,P) EFF1LIB REV1

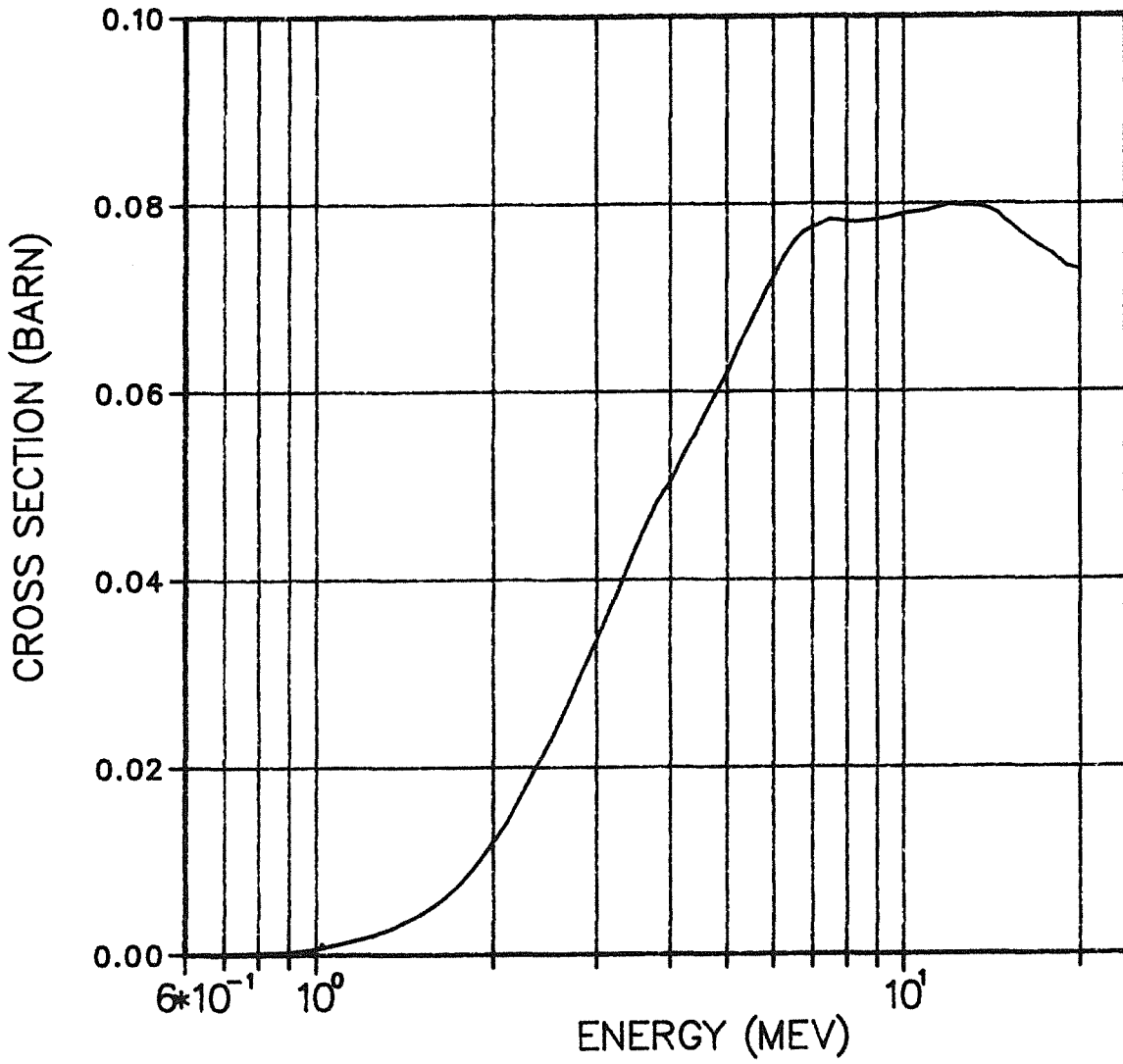


Fig. 6 (n,p)–Cross Section of the Element Iron

PL0T 2 06.46.25 TUES 16 OCT, 1980 JOB-DAR090 , REWFORMSCHUNGSZENTRUM KRWL-SHLEIE DISPLA 10.0

NICKEL 58 (N,P) ENDL-85

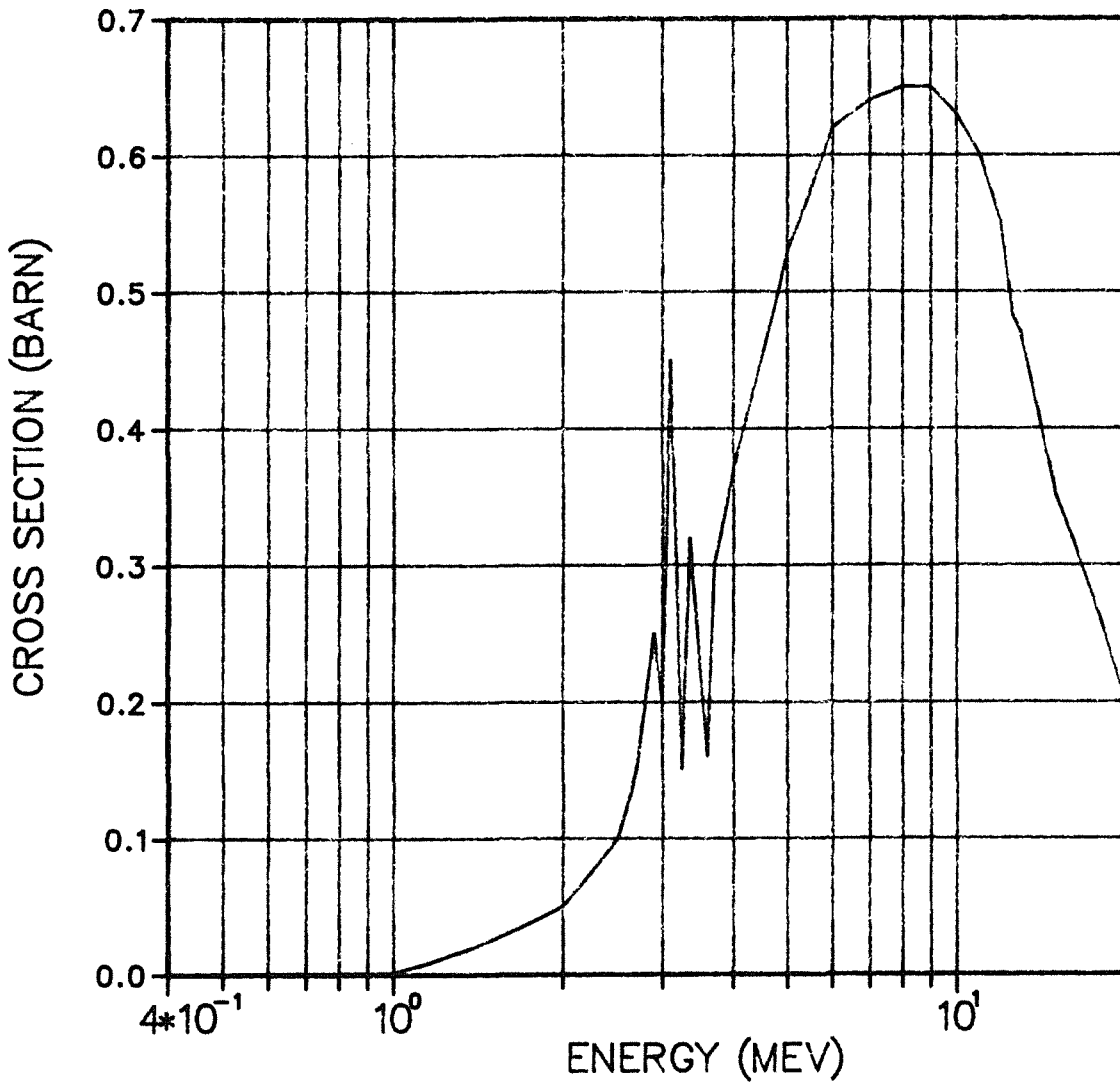


Fig. 7 (n,p)–Cross Section of the Isotope Nickel–58

PL01 3 15.44.18 1125 18 027, 1880 JOB-DK088 , KERNPROZESSDATEN KREISLAUF DTSEP11 10.0

Argon 40 (n,Gamma) LLL-Howerton

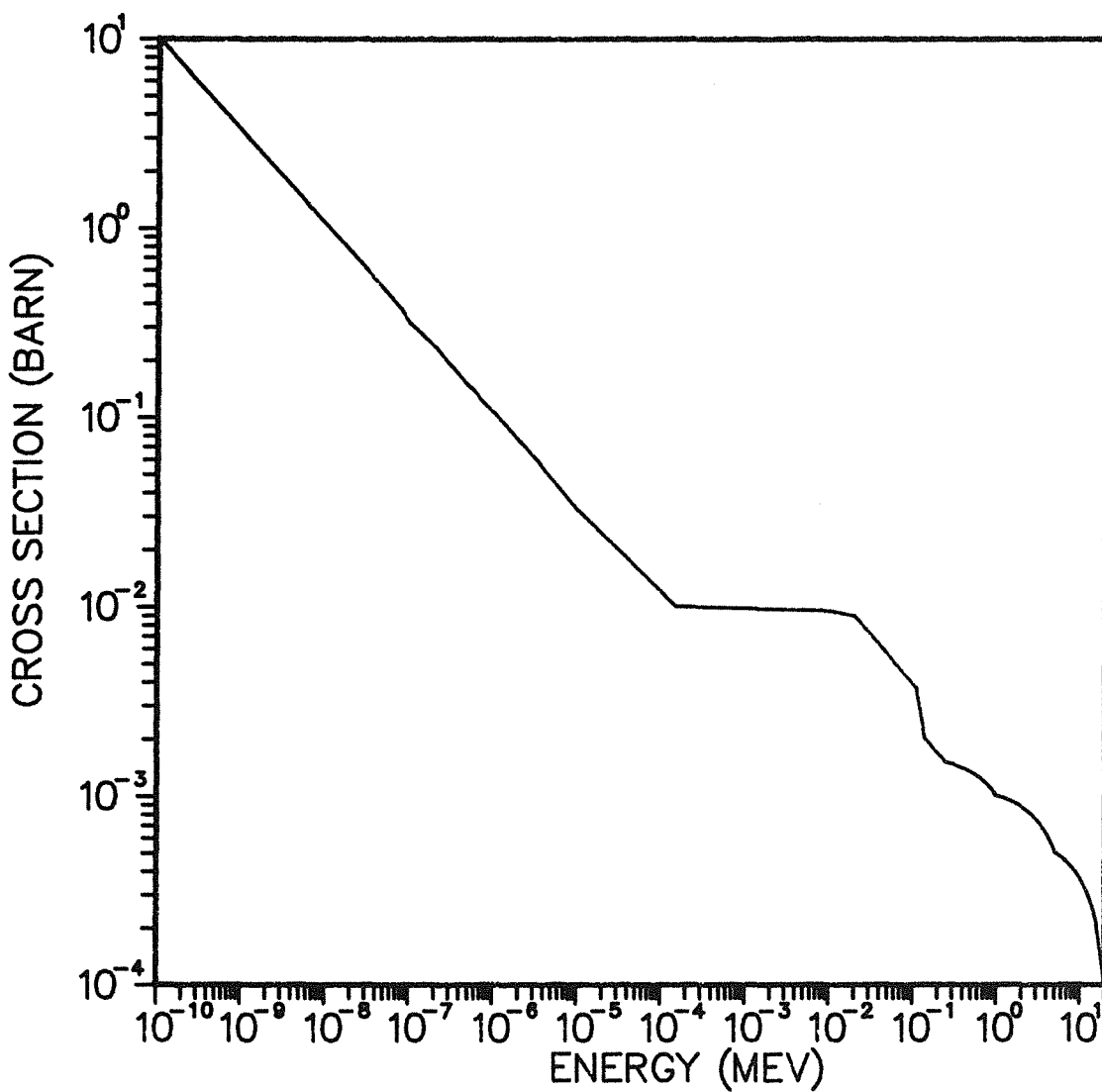


Fig. 8 Radiative Capture Cross Section of Argon-40

PL01 25 08.10.14 10:25 18 Oct, 1960 JOB-114000 , NEWTONSUNSHINECENTRAL PAKL-SUNSHINE DISSEPLA 10.0

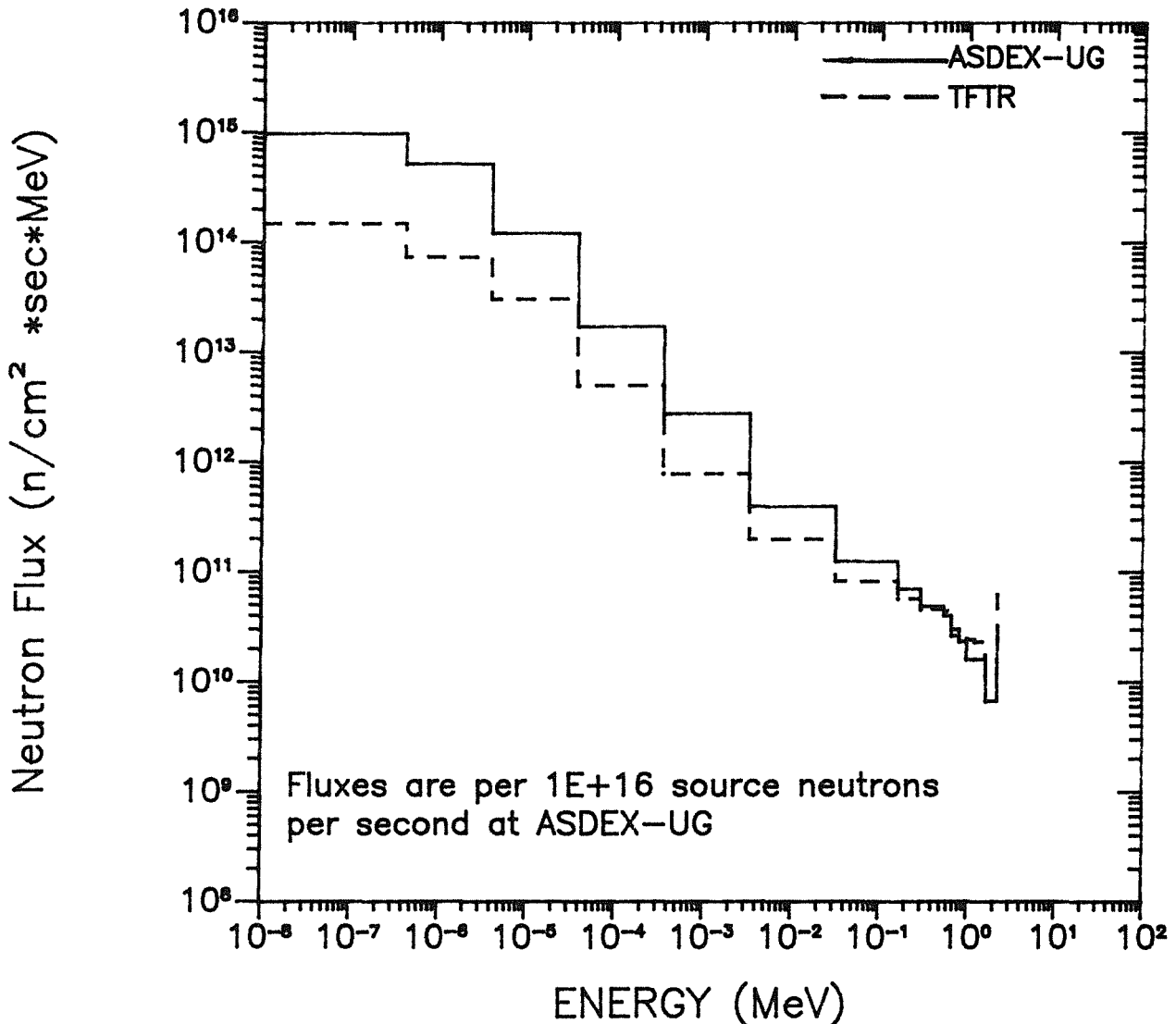


Fig.9 Neutron Flux at the Vacuum Vessel for 2.45 MeV d-d-Neutrons (for Comparison the TFTR Data /5/ are shown, normalized to the ASDEX-UG Data)

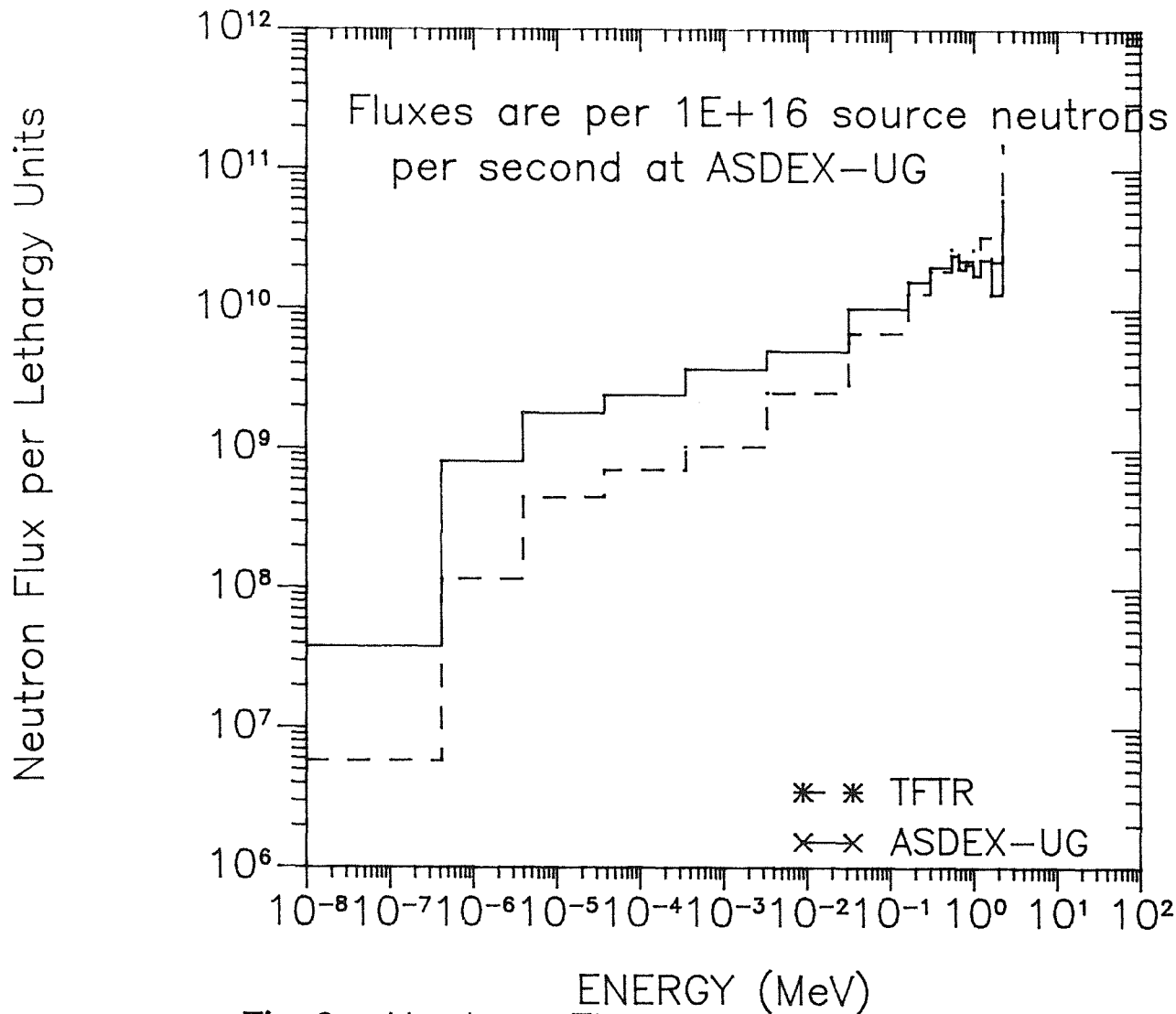


Fig.9a Neutron Flux per Lethargy Units at the Vacuum Vessel for d-d-Neutrons (for Comparison the TFTR Data /5/ are shown, normalized to the ASDEX-UG Data)

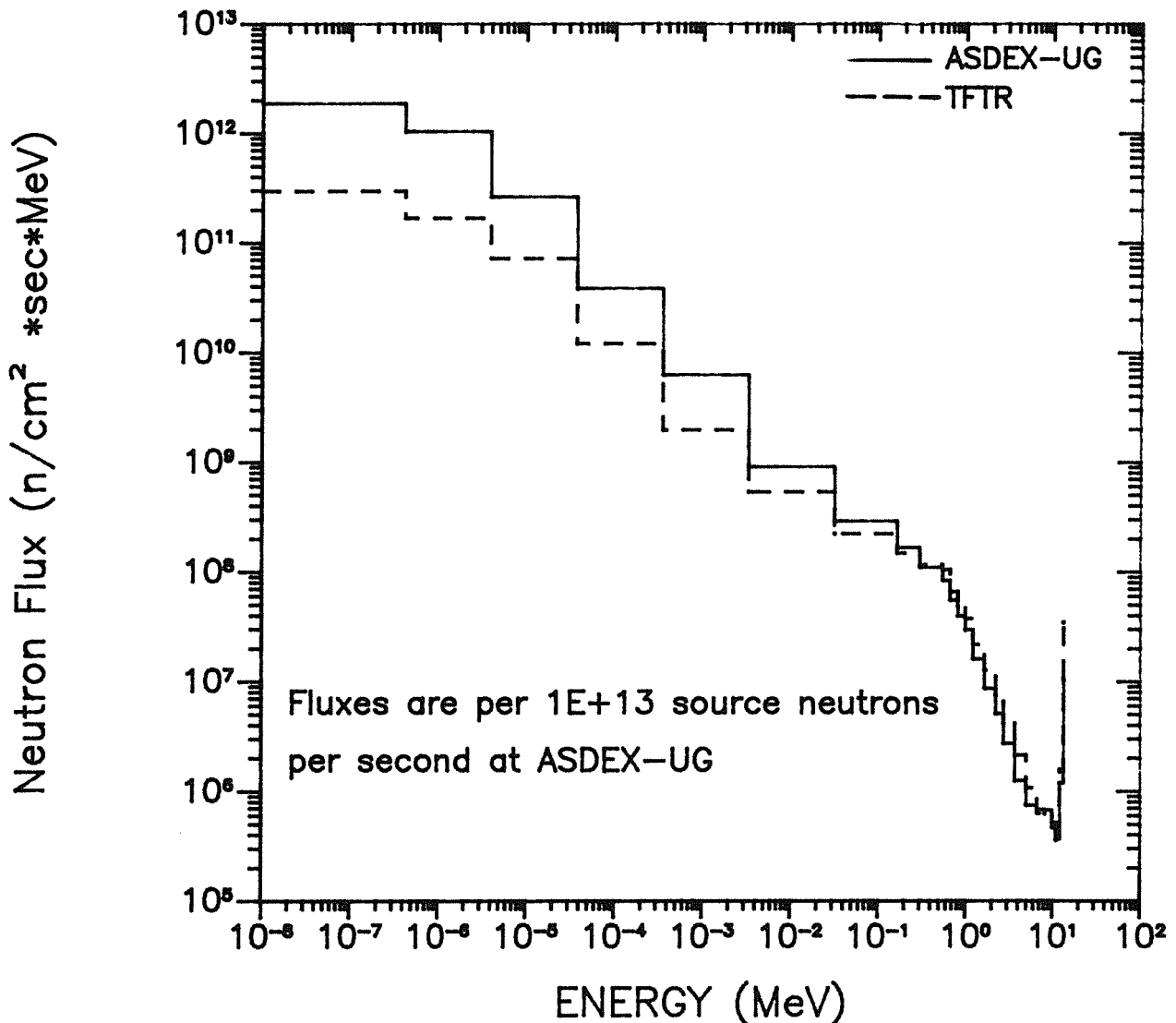


Fig.10 Neutron Flux at the Vacuum Vessel for 14.7 MeV d-t-Neutrons (for Comparison the TFTR Data /5/ are shown, normalized to the ASDEX-UG Data)

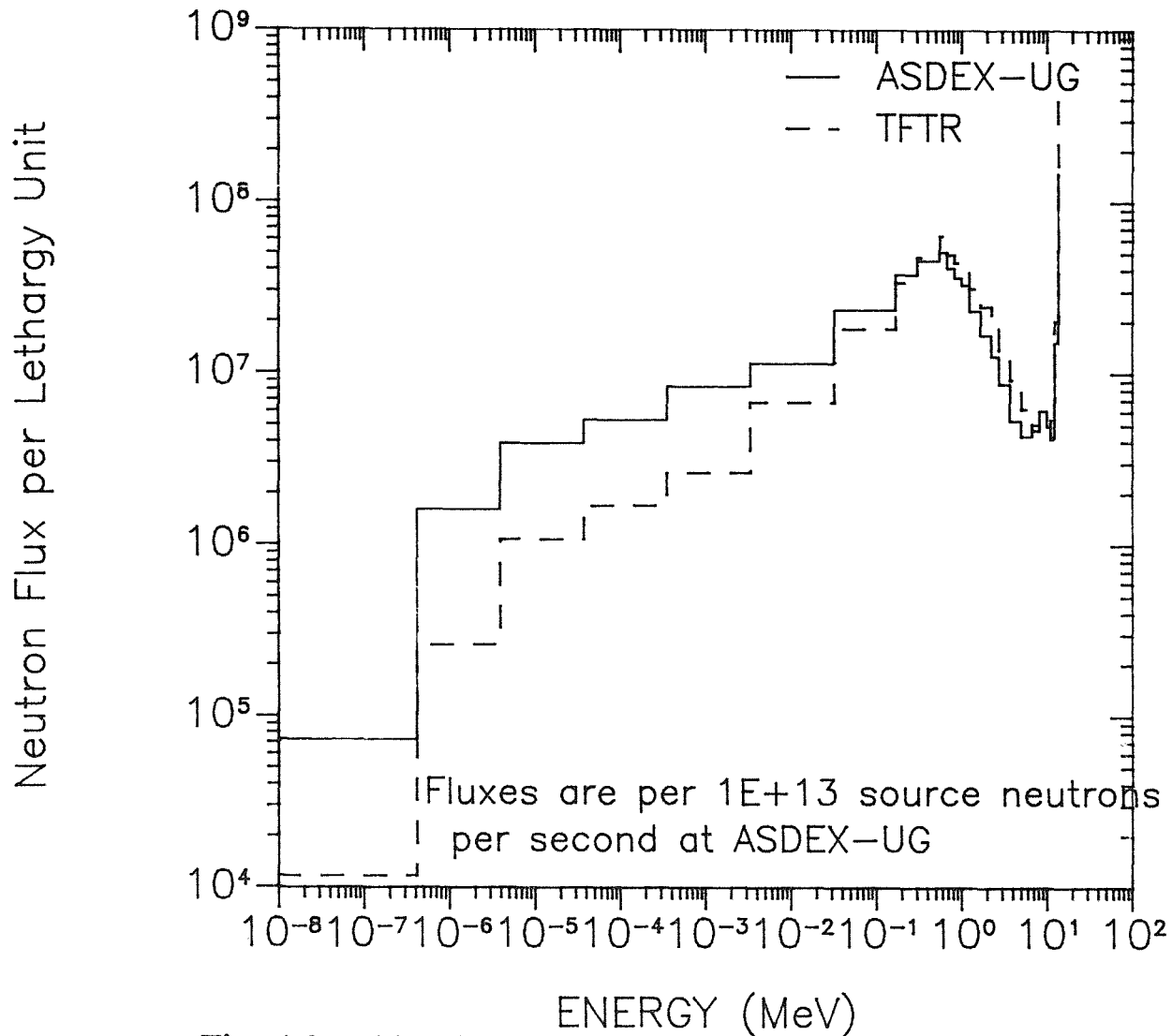


Fig.10a Neutron Flux per Lethargy Units at the Vacuum Vessel for d-t-Source Neutrons [for Comparison the TFTR Data /5/ are shown, normalized to the ASDEX-UG Data]

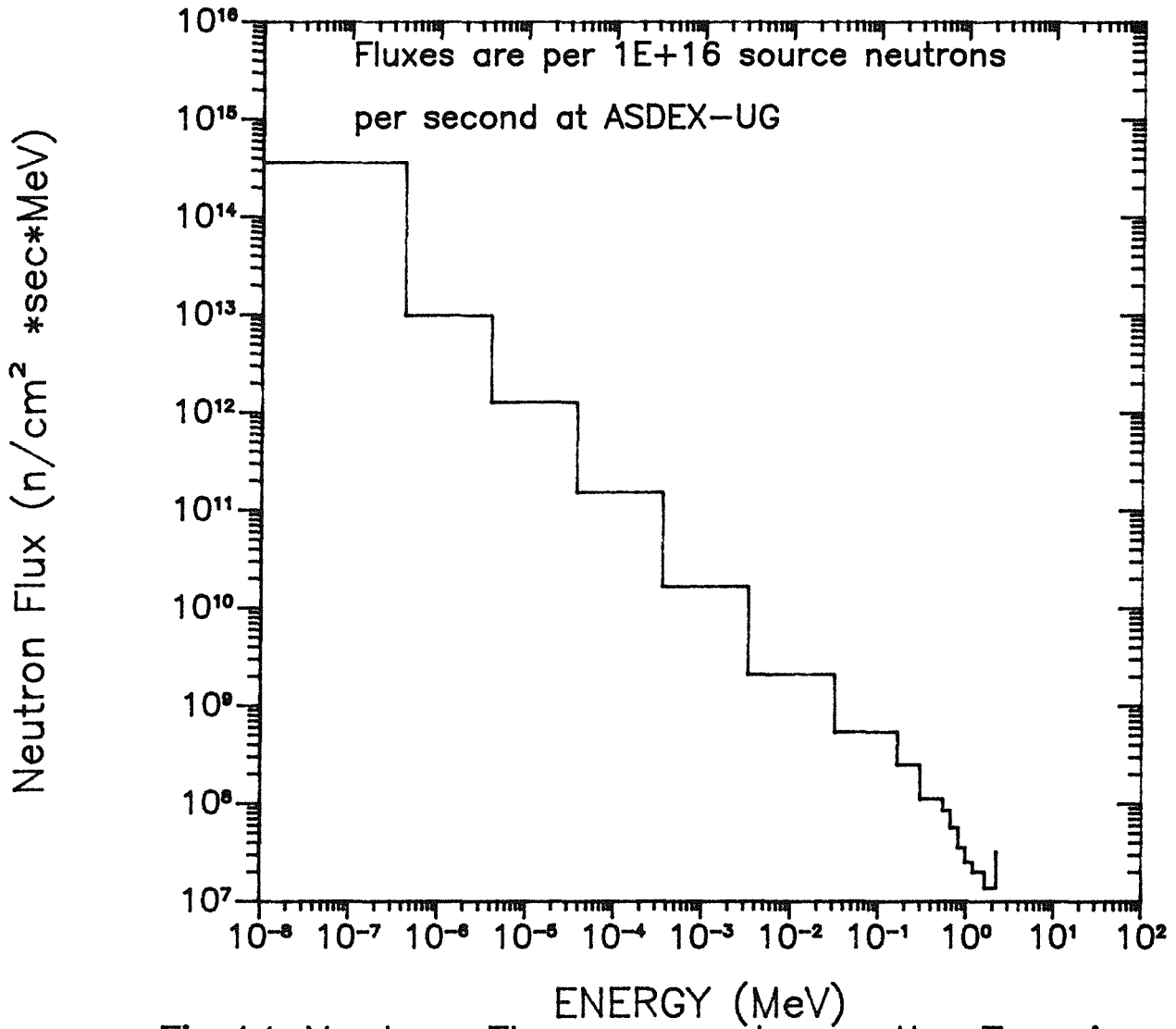


Fig.11 Neutron Flux,averaged over the Experimental Hall for 2.45 MeV d-d-Source Neutrons

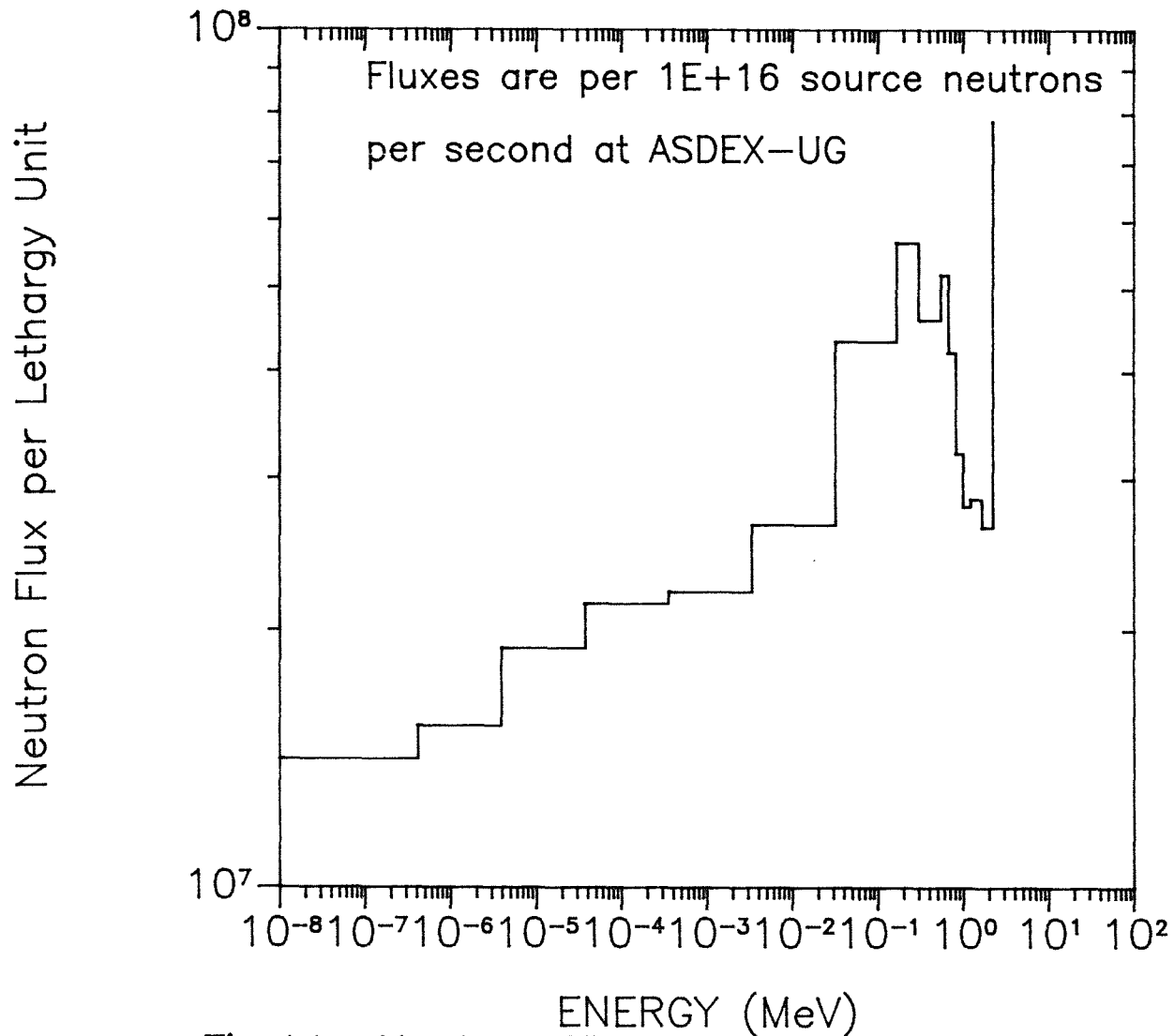


Fig.11a Neutron Flux per Lethargy Units in the Experiment Hall for d-d-Source Neutrons

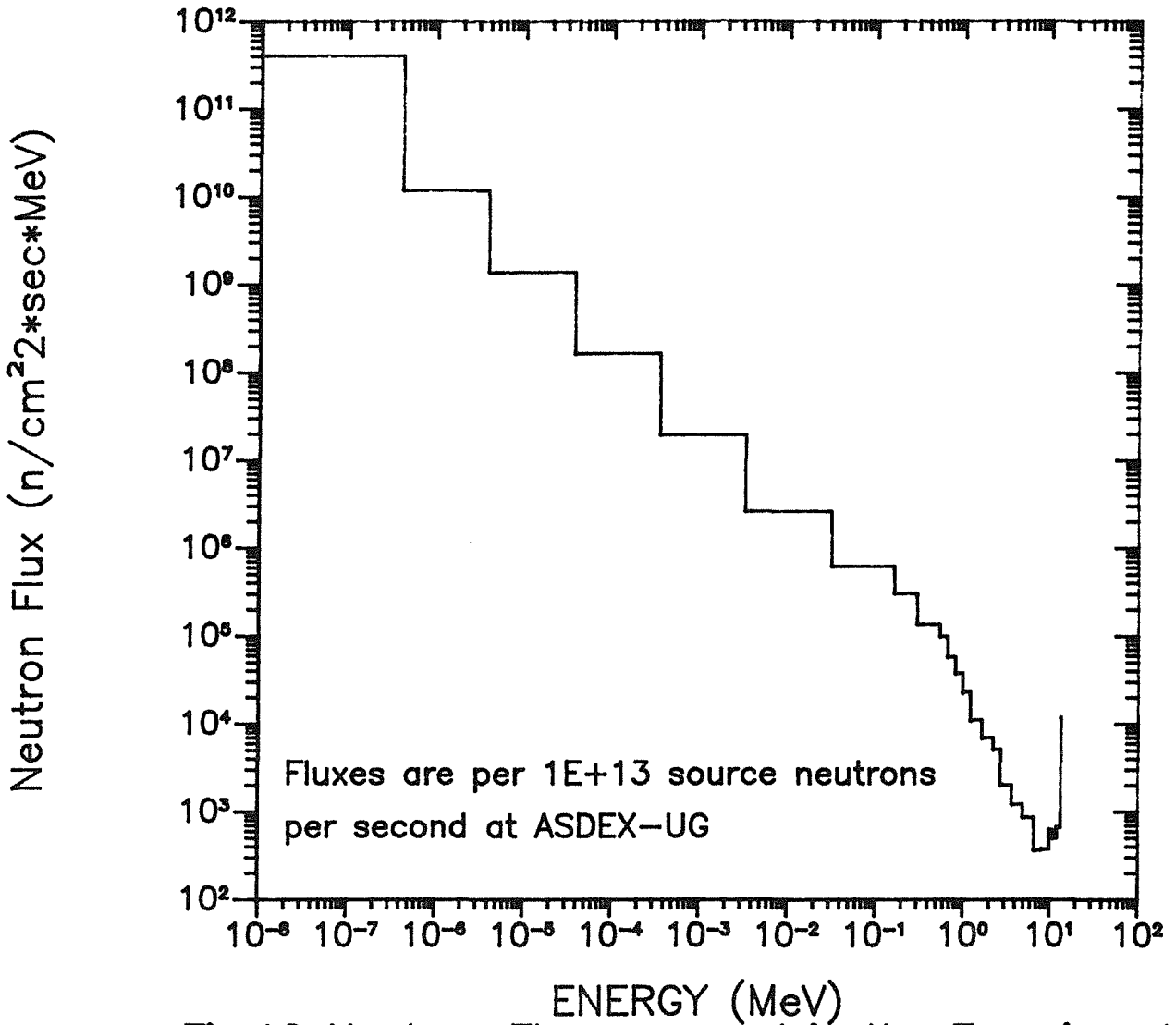


Fig.12 Neutron Flux, averaged in the Experimental Hall for 14.7 MeV d-t-Source Neutrons

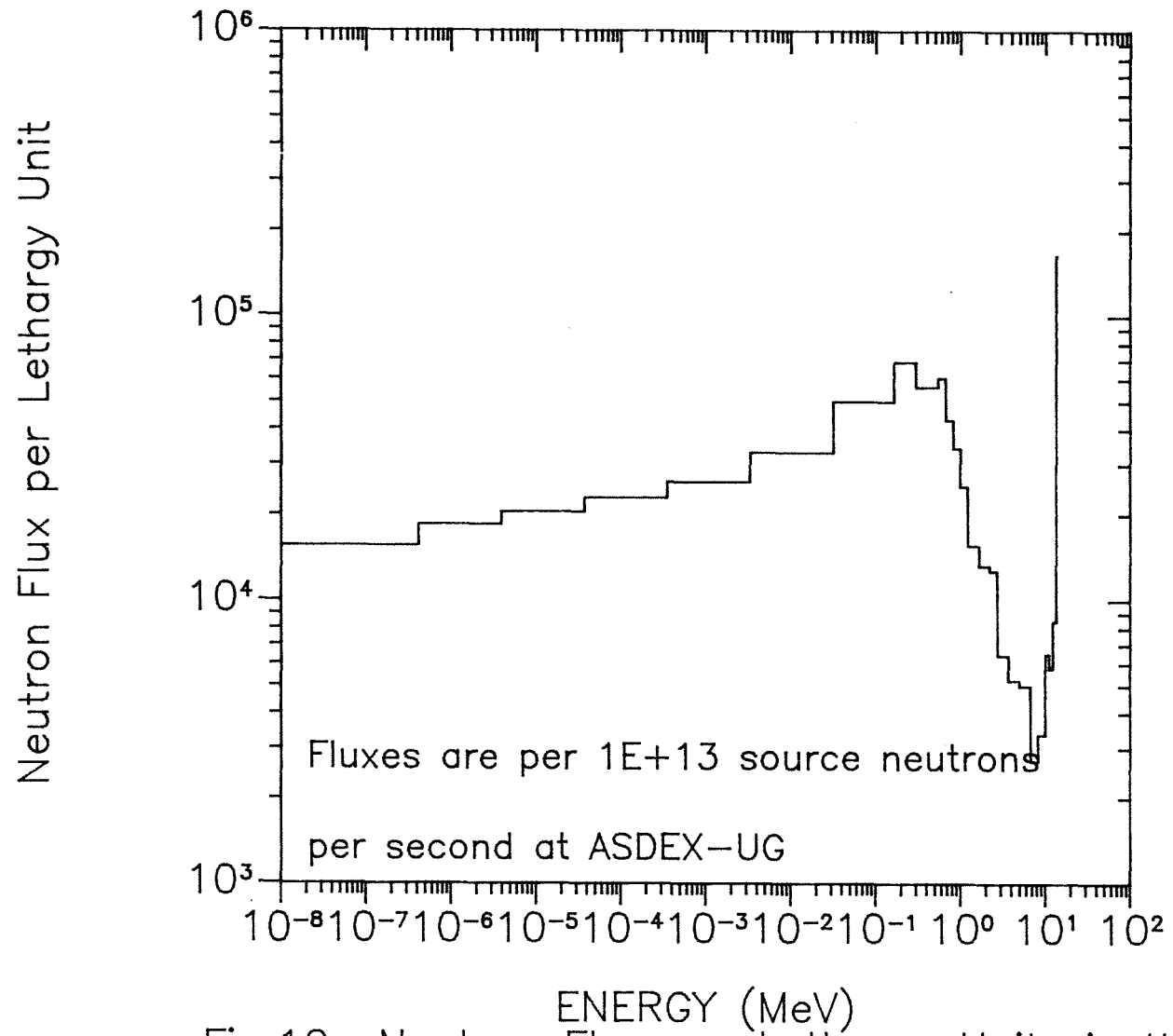


Fig.12a Neutron Flux per Lethargy Units in the Experiment Hall for d-t-Source Neutrons